Electronic Supplementary Material (ESI) for ChemComm.
This journal is © The Royal Society of Chemistry 2019

Rings in Pores-Net: Crown Ether-Based Covalent Organic Frameworks for Phase-Transfer Catalysis

Ji-Chuang Shen,[a] Wei-Ling Jiang,[a] Wen-Di Guo,[a] Qiao-Yan Qi,[b] De-Li Ma,[b] Xiaobing Lou,[c] Ming Shen,[c] Bingwen Hu,[c] Hai-Bo Yang,*[a] and Xin Zhao*[b]

[a] Shanghai Key Laboratory of Green Chemistry and Chemical Processes, School of Chemistry and Molecular Engineering, East China Normal University, Shanghai 200062, China. E-mail: hbyang@chem.ecnu.edu.cn

[b] Key Laboratory of Synthetic and Self-Assembly Chemistry for Organic Functional Molecules, Center for Excellence in Molecular Synthesis, Shanghai Institute of Organic Chemistry, Chinese Academy of Sciences, 345 Lingling Road, Shanghai 200032, China. E-mail: xzhao@sioc.ac.cn

[c] Shanghai Key Laboratory of Magnetic Resonance, School of Physics and Electronic Science, East China Normal University, Shanghai 200062, China

Electronic Supporting Information

Contents

Section 1. General information

1. Materials

All reagents, unless otherwise noted, were purchased from commercial sources in analytical purity and used without further purification. Glass ampoules were dried before used. The internal pressure of the glass ampoule was obtained using a Schlenk line. TLC analyses were performed on silica-gel plates, and flash chromatography was conducted using silica-gel column packages. All solvents were dried according to standard procedures and all of them were degassed under N_2 for 30 minutes before use. All air-sensitive reactions were carried out under argon atmosphere.

2. Instrumentation

N_2 adsorption–desorption isotherms were measured at 77 K with a Micromeritics TriStar II 3020 analyzer. Prior to analysis, the samples were degassed at 100 °C for 12 h. The specific surface areas were calculated according to the Brunauer–Emmett–Teller (BET) method. The Barrett–Joyner–Halenda (BJH) model was utilized to calculate the pore volumes and pore size distributions. Infrared (IR) spectra were obtained using a Bruker tensor 27 infrared spectrometer. The Powder X-ray diffraction (PXRD) patterns were collected on a Rigaku Ultima IV diffractometer using Cu Kα radiation (λ = 0.1542 nm) at 35 kV and 25 mA in the 2θ angle range of 1.5-30º using a step size of 0.02°and at a scanning speed of 10° min^{-1}. The samples were prepared by filling the holder with the dry powder. Scanning electron microscopy (SEM) images of the solutions were obtained using an S-4800 (Hitachi Ltd.) with an accelerating voltage of 10.0 kV. Transmission electron microscopy (TEM) images were recorded on a Tecnai G2 F30 (FEI Ltd.) at 300kV. The samples were dripped on a Holey carbon coated TEM-grid (300 mesh Cu grid, Pacific Grid Tech, USA) after being dispersed in ethanol by ultrasound. Thermogravimetric analyses (TGA) were performed on a Netzsch STA 449 F3 instrument. The sample was heated from 25 to 800 ℃ with the heating rate 10 ℃·min^{-1} under a flow of nitrogen (10 mL·min^{-1}). Solution ^1H and ^{13}C NMR spectra were collected on Bruker 400 MHz NMR spectrometer, Bruker 300 MHz NMR spectrometer or Bruker 500 MHz Spectrometer using tetramethylsilane (TMS) as an internal standard. Solid-state NMR experiments were performed on 9.4T Bruker Bruker AVANCE-III wide bore NMR spectrometer. Samples were packed inside 4mm Zirconium rotors and were spinning at 5 to 8 kHz. The ^{13}C

CP spectra were recorded using a 4mm triple-resonance probe with a recycle delay of 1.5 s, a contact time of 3 ms, and TPPM decoupling of 50 kHz. The rf field for ^{1}H and ^{13}C $\pi/2$ pulses were 100 kHz and 80 kHz respectively. The identification and quantitation of products were performed on a gas chromatograph-mass spectrometer (GC-MS) (SHIMADZU GCMS-QP2020 equipped with a 0.25 mm × 30 m Rtx-5MS capillary column). Elemental analysis was carried out on an PE (PerkinElmer) EA2400 II elemental analyzer. Element concentration was measured by using the Agilent Technology 5100 Series inductively coupled plasma optical emission spectrometry (ICP-OES).

Section 2. Synthesis of crown ether functionalized p-triphenylene diamine (CE-TPDA)

Scheme S1. Synthesis of crown ether functionalized p-triphenylene diamine (**CE-TPDA**)

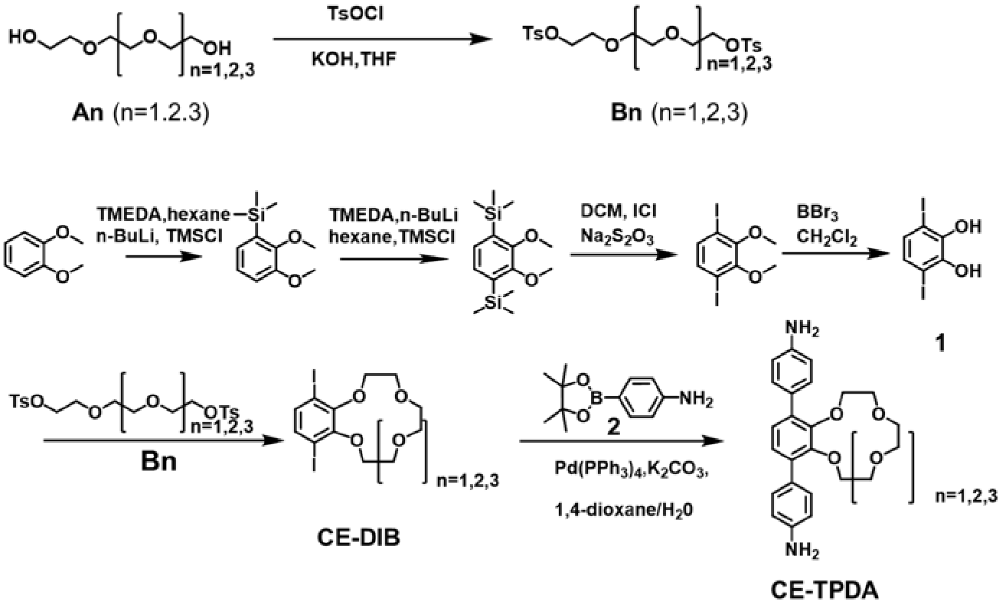

Poly (ethylene glycol) di-*p*-toluenesulfonate (**Bn**) were synthesized according to the method reported in the literature.[1] The obtained ^{1}H spectra of **Bn** matched well with those reported[1] previously. **B1**, ^{1}H NMR (400 MHz, $CDCl_3$): *δ* (ppm) = 7.78 (d, *J* = 8.3 Hz, 4H), 7.33 (d, *J* = 8.0 Hz, 4H), 4.13 (t, *J* = 4.8 Hz, 4H), 3.65 (t, *J* = 4.8 Hz, 4H), 3.52 (s, 4H), 2.44 (s, 6H);**B2**, ^{1}H NMR (400 MHz, $CDCl_3$): *δ* (ppm) = 7.73 (d, *J* = 8.3 Hz, 4H), 7.29 (d, *J* = 8.0 Hz, 4H), 4.10 (t, *J* = 4.4 Hz, 4H), 3.62 (t, *J* = 4.4 Hz, 4H), 3.50 (s, 8H), 2.39 (s, 6H); **B3**: ^{1}H NMR (400 MHz, $CDCl_3$) : *δ* (ppm) = 7.75 (d, *J* = 8.3 Hz, 4H), 7.31 (d, *J* = 8.1 Hz, 4H), 4.12(t, *J* = 4.8 Hz, 4H), 3.64 (t, *J* = 4.8 Hz, 4H), 3.56 (s, 4H), 3.54 (s, 8H), 2.41 (s, 6H).

3,6-diiodobenzene-1,2-diol (**1)** was synthesized according to the reported procedure.[2] The obtained ^{1}H NMR spectra of **1** matched well with those reported previously. ^{1}H NMR (300 MHz, $CDCl_3$): *δ* (ppm) = 7.00 (s, 2H), 5.67 (s, 2H).

These four prepared compounds above were used for the next steps without further characterization.

Crown ether functionalized *p*-diiodobenzene (**CE-DIB**) were obtained through the Williamson reaction between poly (ethylene glycol) di-*p*-toluenesulfonate **Bn** and 3,6-diiodobenzene-1,2-diol (**1**), The general experimental procedures are as follows:

1 (5.5 mmol), K_2CO_3 (3.8 g, 5.0 equiv.), template molecule (0.5 equiv.; LiI for **12C4-DIB,** Na_2CO_3 for **15C5-DIB,** K_2CO_3 for **18C6-DIB**) were added to a 500 mL three-necked flask with a magneton. and the flask was evacuated and refilled with N_2 three times, and 200 mL CH_3CN was injected. **Bn** (1.1 equiv.) in CH_3CN (100 mL) was added dropwise over a period of 2h at 70 ℃ and the mixture was stirred at the same temperature for a further 48 h, then allowed to cool to room temperature, and filtered through diatomite. The filtrate was concentrated to dryness under vacuum. The crude product was purified by flash column chromatography on silica gel to give the product **CE-TPDA**.

12C4-DIB: The crude product was purified by column chromatography with hexane/ethyl acetate (5:1) as eluent to afford the title compound **12C4-DIB** as white solid. Yield: (61.5%). ^{1}H NMR (300 MHz, $CDCl_3$): δ (ppm) = 7.26 (s, 2H), 4.20 (t, J =4.1, 4H), 3.94 (t, J =4.1, 4H), 3.81 (s, 4H). ^{13}C NMR (126 MHz, $CDCl_3$): δ (ppm) = 153.03, 135.95, 93.64, 73.43, 71.10， 70.71. HRMS (ESI): Calculated for $C_{12}H_{15}O_4I_2$ $[M + H]^+$: 476.9060, found: 476.9056. Mp: 151.1 ℃.

15C5-DIB: The crude product was purified by column chromatography with hexane/ethyl acetate (3:1) as eluent to afford the title compound **15C5-DIB** as white solid. Yield: (69.6%). ^{1}H NMR (300 MHz, $CDCl_3$): δ (ppm) = 7.24 (s, 2H), 4.20 (t, J = 5.2 Hz, 4H), 4.01 (t, J = 5.2 Hz, 4H), 3.74 (s, 8H). ^{13}C NMR (126 MHz, $CDCl_3$): δ (ppm) = 152.70, 135.68, 93.36 ,72.90, 71.27, 70.67, 70.43. HRMS (ESI): Calculated for $C_{14}H_{19}O_5I_2$ $[M + H]^+$: 520.9322; Found: 520.9315, Mp: 117.4 ℃.

18C6-DIB: The crude product was purified by column chromatography with hexane/ethyl acetate (2:1) as eluent to afford the title compound **18C6-DIB** as white solid. Yield: (80.0%). ^{1}H NMR (300 MHz, $CDCl_3$): δ (ppm) = 7.23 (s, 2H), 4.22 (t, J = 5.0 Hz, 4H), 3.98 t, J = 5.0 Hz, 4H), 3.75 (s, 8H), 3.69 (s, 4H). ^{13}C NMR (126 MHz, $CDCl_3$): δ (ppm) = 152.51, 135.64, 93.33, 73.09, 71.03, 70.82, 70.42. HRMS (ESI): Calculated for $C_{16}H_{23}O_6I_2$ $[M+ H]^+$: 564.9584; Found: 564.9577. Mp: 83.5 ℃.

Crown ether functionalized p-triphenylene diamine building blocks (**CE-TPDA**) were obtained through the Suzuki coupling reaction between **CE-DIB** and **1**. The general experimental procedures are as follows:

CE-DIB (4.2 mmol), K_2CO_3 (2.8 g, 5.0 equiv.), 4-(4,4,5,5-tetramethyl-1,3,2-dioxaborolan-2-yl) aniline **2** (2.3 g, 2.5 equiv.), and $Pd(PPh_3)4$ (473 mg, 0.1 equiv.) were added into a two-necked flask. A degassed mixture of 1,4-dioxane (20mL) and H_2O (5 mL) was added into the flask under N_2 atmosphere. The reaction mixture was heated to reflux at 100 °C for 24 h. After cooling to room temperature, the solvent was evaporated under reduced pressure and the residue was diluted with H_2O (20 mL), extracted with CH_2Cl_2 (3 × 50 mL). The combined organic layer was washed with brine, dried over Na_2SO_4, and then evaporated to dryness. The crude product was purified by flash column chromatography on silica gel to give the product **CE-TPDA**.

12C4-TPDA: The crude product was purified by flash column chromatography on silica gel with hexane/ethyl acetate (2:1) as the eluent to give the product **12C4-TPDA** as an off-white solid. Yield: 1.0 g (60.4%). ^{1}H NMR (400 MHz, DMSO): δ (ppm) = 7.25 (d, J = 8.5 Hz, 4H), 7.02 (s, 2H), 6.62 (d, J = 8.5 Hz, 4H), 5.22 (s, 4H), 3.88 – 3.78 (m, 4H), 3.64 (s, 4H), 3.64 – 3.60 (m, 4H). ^{13}C NMR (126 MHz, DMSO): δ (ppm) = 150.17, 148.19, 134.62, 129.81, 125.57, 125.22, 114.20, 72.80, 70.57, 70.01. HRMS (EI): Calculated for $C_{24}H_{26}O_4N_2$ $[M]^+$: 406.1893; Found: 406.1896. Mp: 164.7 ℃.

15C5-TPDA: The crude product was purified by flash column chromatography on silica gel with hexane/ethyl acetate (1:1) as the eluent to give the product **15C5-TPDA** as a light-brown solid. Yield: 1.4 g (71.8%).^{1}H NMR (300 MHz, DMSO): δ (ppm) = 7.24 (d, J = 8.5 Hz, 4H), 7.01 (s, 2H), 6.62 (d, J = 8.5 Hz, 4H), 5.21 (s, 4H), 3.82 (t, J = 4.8 Hz, 4H), 3.65 (t, J = 4.8 Hz, 4H), 3.57 (s, 8H). ^{13}C NMR (126 MHz, DMSO): δ (ppm) = 150.16 , 148.21, 134.52, 129.83, 125.56, 125.12, 114.15, 72.56, 70.81, 70.09, 69.95. HRMS (EI): Calculated for $C_{26}H_{30}O_5N_2$ $[M]^+$: 450.2155; Found: 450.2158. Mp: 146.6 ℃.

18C6-TPDA: The crude product was purified by flash column chromatography on silica gel with ethyl acetate as the eluent to give the product **18C6-TPDA** as a light-brown solid. Yield: 1.7 g (81.2%).^{1}H NMR (500 MHz, DMSO): δ (ppm) = 7.24 (d, J = 8.5 Hz, 4H), 7.01 (s, 2H), 6.61 (d, J = 8.5 Hz, 4H), 5.17 (s, 4H), 3.82 (t, J = 5.2 Hz, 4H), 3.60 (t, J = 5.2 Hz, 4H), 3.58 – 3.52 (m, 12H). ^{13}C NMR (126 MHz, DMSO): δ (ppm) = 149.53, 147.84, 134.03, 129.40, 124.92, 124.68, 113.58, 71.89, 70.10, 69.86, 69.74, 69.57. HRMS (EI): Calculated for $C_{28}H_{34}O_6N_2$ $[M]^+$: 494.2417; Found: 494.2423. mp: 62.1 ℃.

Section 3. Synthesis, characterization, and structural modeling of 12C4-COF

1. Synthesis of 12C4-COF

Scheme S2. Synthesis of **12C4-COF** by condensation of **12C4-TPDA** and 1,3,5-Triformylbenzene

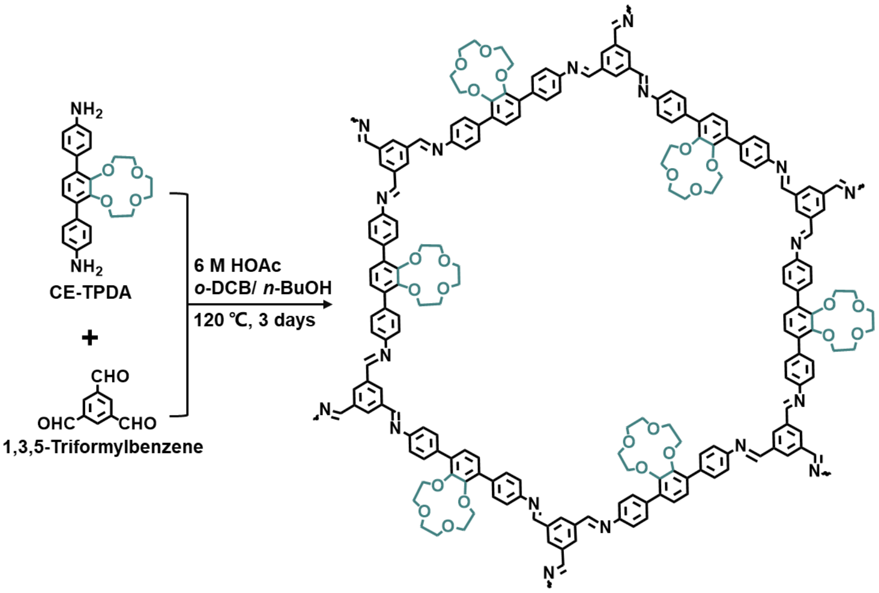

1,3,5-Triformylbenzene (19.46 mg, 0.12 mmol) and **12C4-TPDA** (73.16 mg, 0.18 mmol) were weighed into a 10 mL pressure ampoule (body length of 18 cm and neck length of 9 cm). To the mixture were added *o*-dichlorobenzene ***o*-DCB** (0.2 mL), *n*-BuOH (0.8 mL), and 6 M aqueous acetic acid (0.2mL). Then the ampoule was flash frozen in a liquid nitrogen bath, evacuated to an internal pressure of 0.1 Pa and flame sealed, reducing the total length by *ca.* 10 cm. After warming to room temperature, the sealed ampoule was placed in an oven at 120 °C and left undisturbed for 3 days, yielding a yellow solid. The ampoule was opened when the mixture was still warm (over 40 °C) and the solid was transferred into a 10mL centrifuge-tube, separated by centrifugation, washed with DMF (3 × 8 mL), THF (3 × 8 mL) and acetone (3 × 8 mL). The resulting solid was further dried under vacuum at 100 °C for 12 hours, to yield **12C4-COF** as a yellow powder (70.8 mg, 82.2% yield). Further purification of **12C4-COF** was carried out by Soxhlet extraction in THF for 12 h. Anal. Cald. for $(C_{15}H_{13}O_2N)_n$: C 73.31; H 5.44; N 5.85. Found: C 73.25; H 5.56; N 5.35.

2. Characterization of 12C4-COF

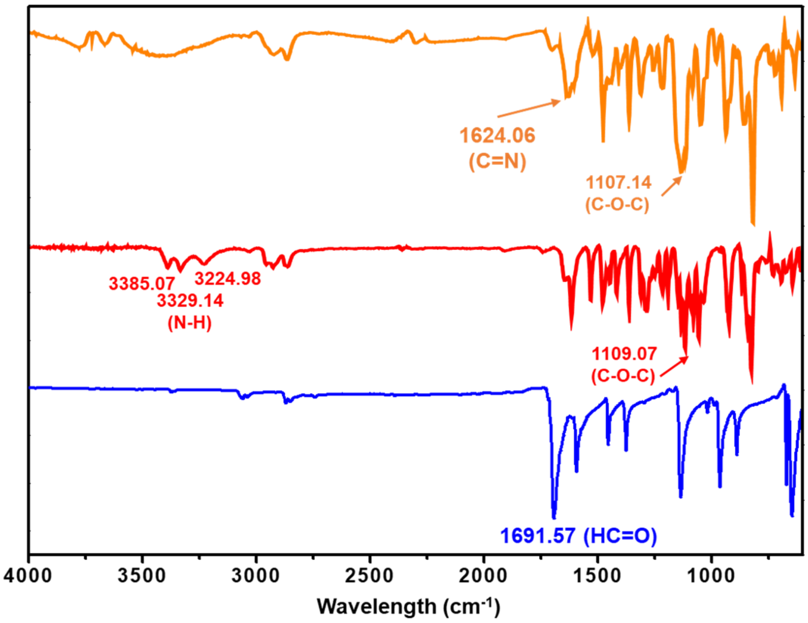

Figure S1. FT-IR spectra of **12C4-COF** (orange), **12C4-TPDA** (red) and 1,3,5-Triformylbenzene (blue).

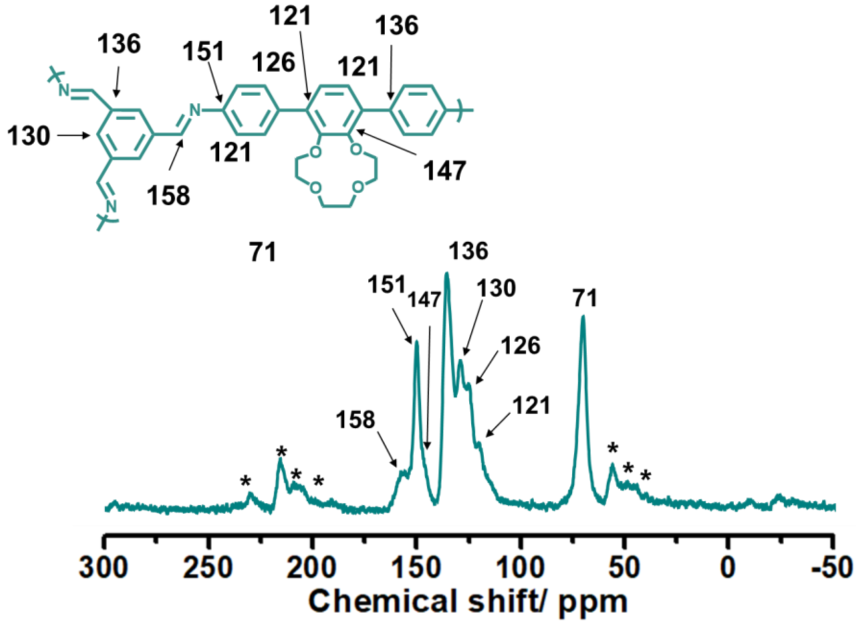

Figure S2. ^{13}C CP/MAS NMR spectrum of **12C4-COF**. The asterisks denote the spinning sidebands. The MAS spinning speed was 8 kHz.

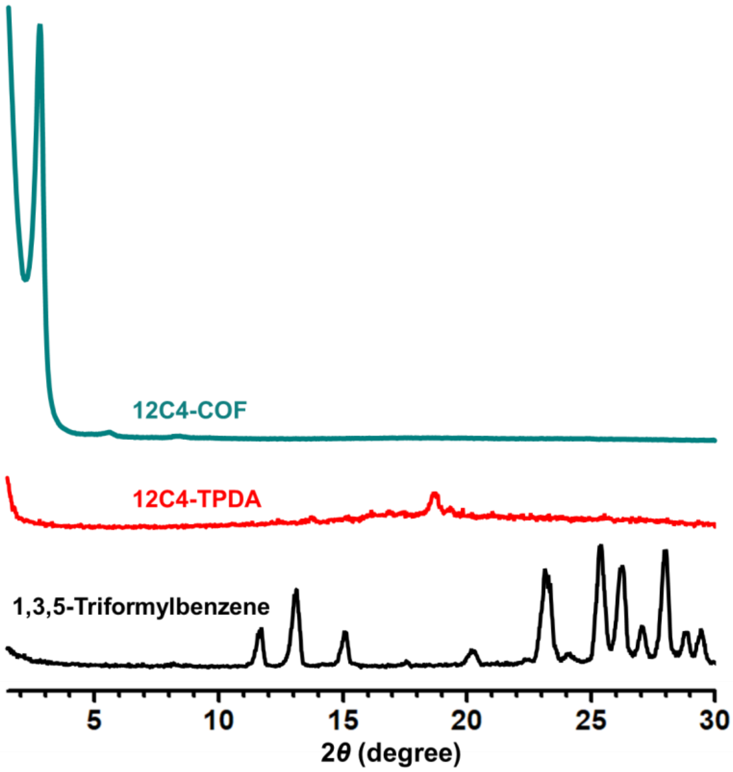

Figure S3. PXRD patterns of **12C4-COF** (sky blue), **12C4-TPDA** (red), and 1,3,5-Triformylbenzene (black).

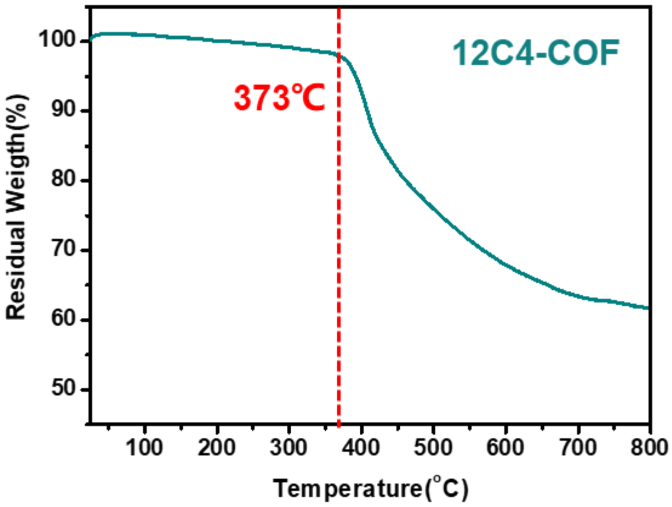

Figure S4.TGA data of **12C4-COF. 12C4-COF** is thermally stable up to 373 °C.

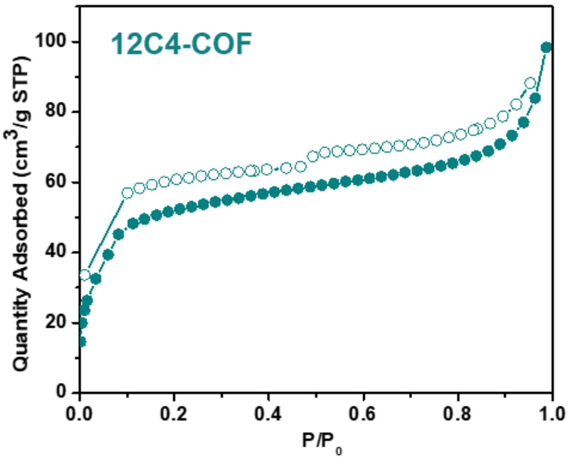

Figure S5. Nitrogen adsorption (filled symbols) and desorption (empty symbols) isotherms of **12C4-COF**. The profile showed a type-IV isotherm, which is characteristic for a mesoporous material.

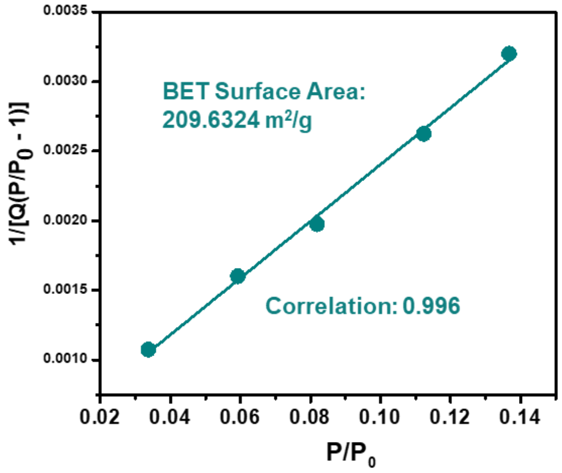

Figure S6. BET surface area plot for **12C4-COF** calculated from the absorption isotherm.

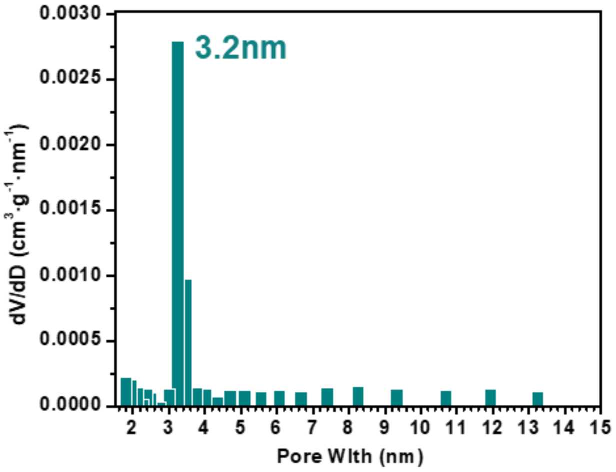

Figure S7. Pore size distribution of **12C4-COF** calculated by BJH method.

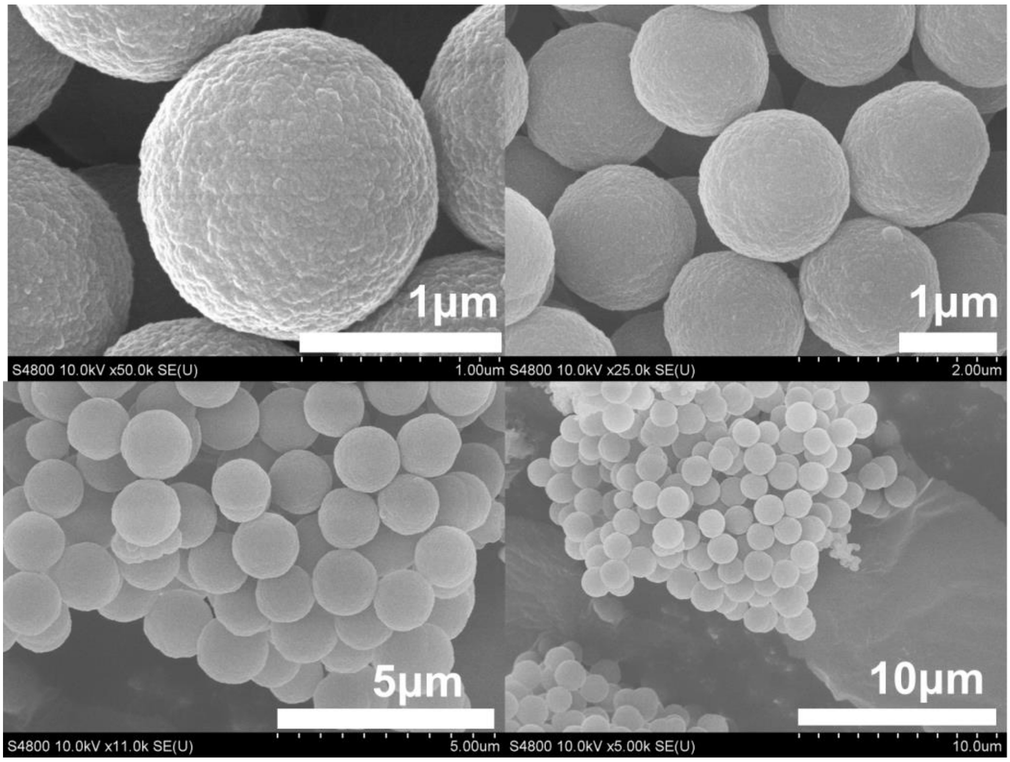

Figure S8. SEM image of **12C4-COF**. The image showed that **12C4-COF** adopted a sphere-like morphology with an average particle size of *ca.* 1 µm.

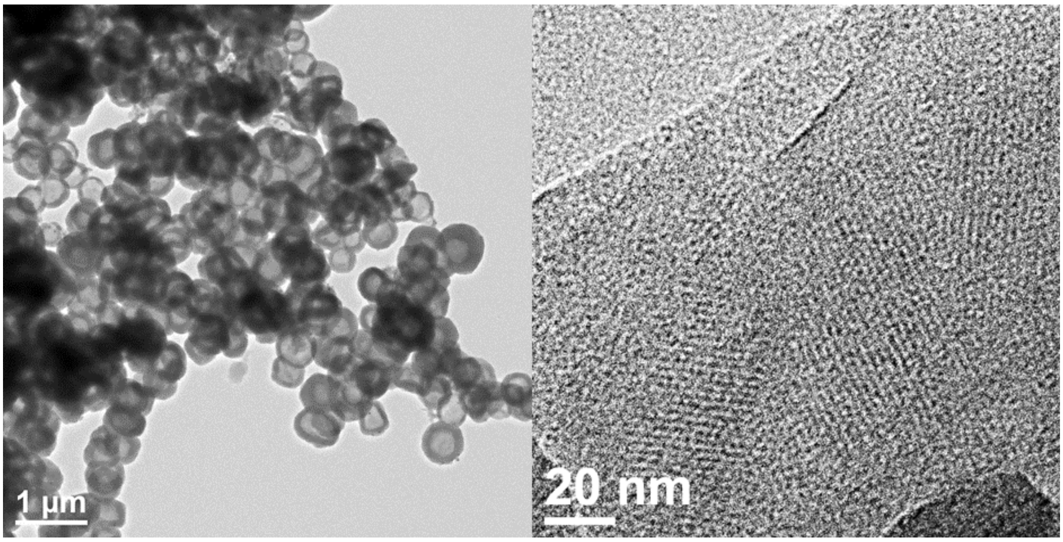

Figure S9. TEM image of **12C4-COF**

3. Structural modeling and Powder X-Ray Diffraction analyses of 12C4-COF

The simulations of the possible structures were carried out in Accelrys Material Studio 7.0 software package. The stimulated PXRD patterns were determined by the Reflex module. The initial space groups for the simulated structures were selected as P3. Pawley refinement of the experimental PXRD of **12C4-COF** was conducted to optimize the lattice parameters iteratively until the R_{wp} value converges, resulting in the cell parameters of a = b = 37.15763 ± 0.42631 Å, c = 4.35598 ± 0.05054 Å, α = β = 90° , and γ = 120° with R_{wp} = 2.38%, and R_p = 1.55%. A staggered arrangement (AB) for **12C4-COF** was also constructed with the space group P3, Comparison of the observed and the simulated PXRD patterns (Figure S10) suggested that the preferable structure of **12C4-COF** is the eclipsed arrangement (AA).

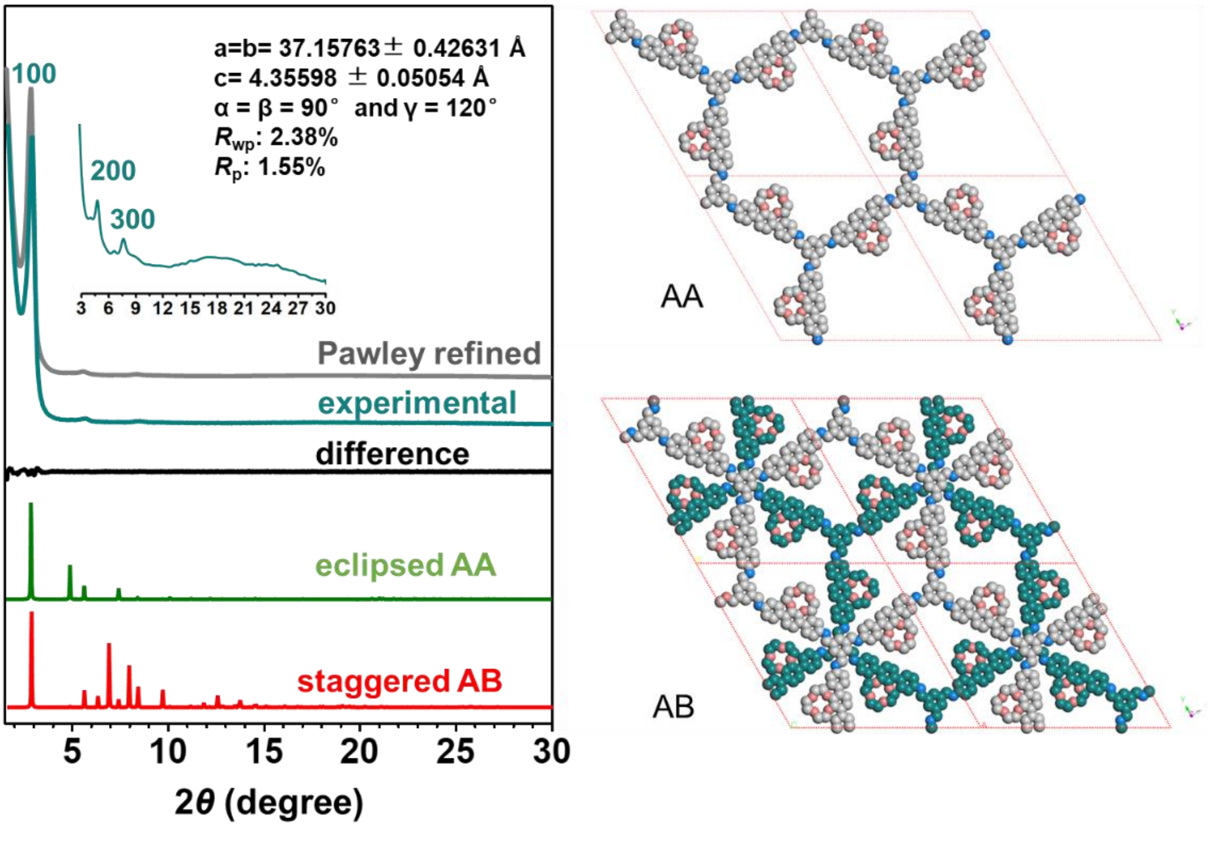

Figure S10. Left: PXRD patterns of **12C4-COF** observed (sky blue), Pawley refined patterns (light gray), difference plot between the observed and refined patterns (black) and calculated with the eclipsed AA (green) or staggered AB (red) stacking models. Right: Graphic views of AA (top) or AB (bottom) models. Comparison of the observed and the simulated PXRD patterns suggested that the preferable structure of **12C4-COF** is the eclipsed arrangement.

Table S1. Fractional atomic coordinates for the unit cell of **12C4-COF** with AA stacking

P3, a = b = 37.15763 ± 0.42631 Å; c = 4.35598 ± 0.05054 Å α = β = 90° and γ = 120°							
Atom	x	y	z	Atom	x	y	z
C1	1.29122	1.6362	0.92339	C32	1.57599	1.91723	0.99115
C2	1.30262	1.67836	0.92429	C33	1.97594	2.01935	1.52629
C3	1.31014	1.58008	0.94588	C34	1.95629	1.97573	1.52478
C4	1.22504	1.42069	1.04954	C35	1.91054	1.94971	1.51095
C5	1.2601	1.45045	1.213	N36	1.88788	1.96558	1.42655
C6	1.27652	1.49295	1.16262	H37	1.25858	1.61273	0.92984
C7	1.25751	1.50703	0.95368	H38	1.33441	1.57268	0.99035
C8	1.22204	1.47787	0.7962	H39	1.27426	1.44138	1.38932
C9	1.20652	1.43527	0.83771	H40	1.30284	1.51469	1.29879
N10	1.27183	1.55051	0.91281	H41	1.20688	1.48821	0.63531
C11	1.65069	1.81365	1.09205	H42	1.18011	1.41385	0.7009
C12	1.69298	1.83683	1.15533	H43	1.63797	1.78114	1.03659
C13	1.71116	1.87832	1.24798	H44	1.71164	1.822	1.13529
C14	1.68611	1.89686	1.27571	H45	1.59326	1.87528	0.7842
C15	1.64369	1.87415	1.1934	H46	1.63547	1.92754	0.81115
C16	1.62511	1.83151	1.10799	H47	1.75517	1.85711	1.63588
C17	1.75648	1.90164	1.30943	H48	1.83045	1.89336	1.71346
O18	1.70159	1.93522	1.42749	H49	1.84488	1.98733	1.06475
O19	1.6201	1.89383	1.2193	H50	1.76977	1.94934	0.97175
C20	1.60774	1.90308	0.93321	H51	1.70781	1.9627	0.98985
C21	1.77451	1.88557	1.51072	H52	1.75049	1.98925	1.25232
C22	1.81764	1.90611	1.55224	H53	1.71902	2.03009	1.22848
C23	1.84346	1.94322	1.39258	H54	1.70578	2.005	1.5946
C24	1.82539	1.95922	1.19329	H55	1.66451	2.02277	0.94365
C25	1.78246	1.93811	1.14606	H56	1.65456	2.03512	1.32685
C26	1.71613	1.97102	1.23459	H57	1.59454	2.01213	0.98648
C27	1.70005	1.99943	1.34469	H58	1.58153	1.97735	1.29769
O28	1.65686	1.98059	1.28921	H59	1.56819	1.91477	1.24021
C29	1.64703	2.00951	1.16096	H60	1.54641	1.89506	0.87554
C30	1.60074	1.98823	1.08564	H61	1.95742	2.03444	1.52359
O31	1.58989	1.95697	0.86031	H62	1.89652	1.91667	1.55046

Section 4. Synthesis, characterization, and structural modeling of 15C5-COF

1. Synthesis of 15C5-COF

Scheme S3. Synthesis of **15C5-COF** by condensation of **15C5-TPDA** and 1,3,5-Triformylbenzene

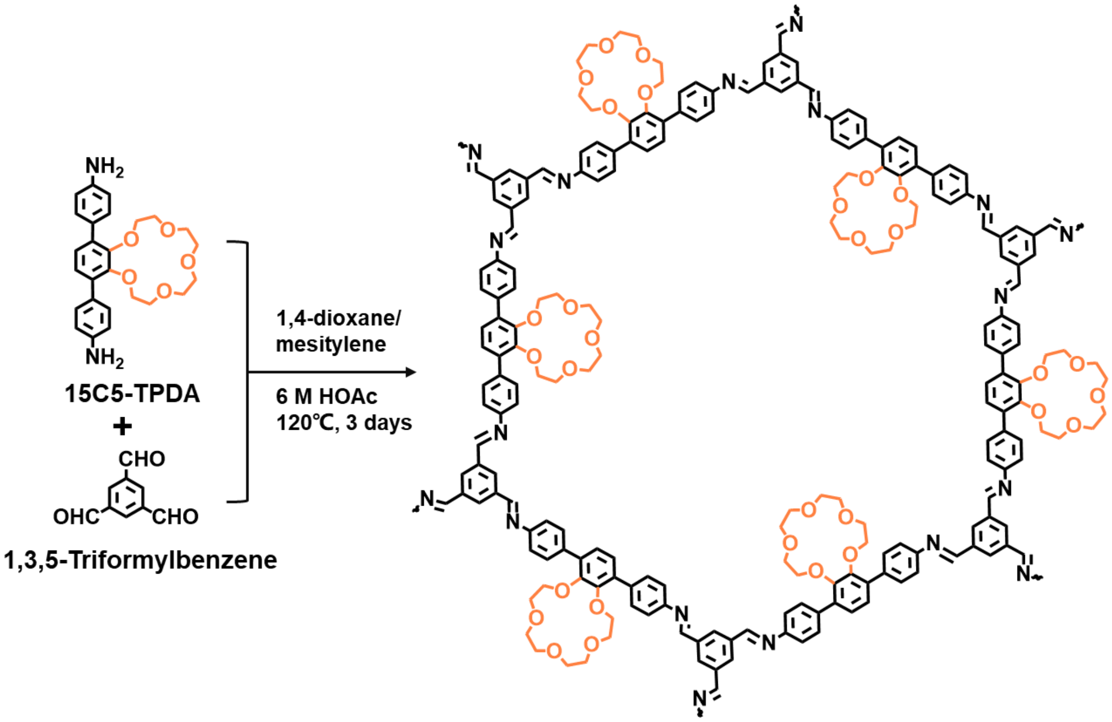

1,3,5-Triformylbenzene (19.46 mg, 0.12 mmol) and **15C5-TPDA** (81.1 mg, 0.18 mmol) were weighed into a 10 mL pressure ampoule (body length of 18 cm and neck length of 9 cm). To the mixture were added 1,4-dioxane (0.15 mL), mesitylene (1.35 mL), and 6 M aqueous acetic acid (0.3mL), it is worth noting that the solvent could also be *o*-dichlorobenzene ***o*-DCB** (0.2 mL) and *n*-BuOH (0.8 mL). Then, the mixture was flash frozen in a liquid nitrogen bath, evacuated to an internal pressure of 0.1 Pa and flame sealed, reducing the total length by *ca.* 10 cm. After warming to room temperature, the sealed ampoule was placed in an oven at 120 °C and left undisturbed for 3 days, yielding a yellow solid. The ampoule was opened when the mixture was still warm (over 40 °C) and the solid was transferred into a 10mL centrifuge-tube, separated by centrifugation, washed with DMF (3 × 8 mL), THF (3 × 8 mL) and acetone (3 × 8 mL). The resulting solid was further dried under vacuum at 100 °C for 12 hours, to yield **15C5-COF** as a yellow powder (80.9 mg, 86.1% yield). Further purification of **15C5-COF** was carried out by Soxhlet extraction in THF for 12 h. Anal. Cald for $(C_{16}H_{15}O_{2.5}N)_n$: C 73.56; H 5.75; N 5.36. Found: C 70.99; H 5.86; N 4.76.

2. Characterization of 15C5-COF

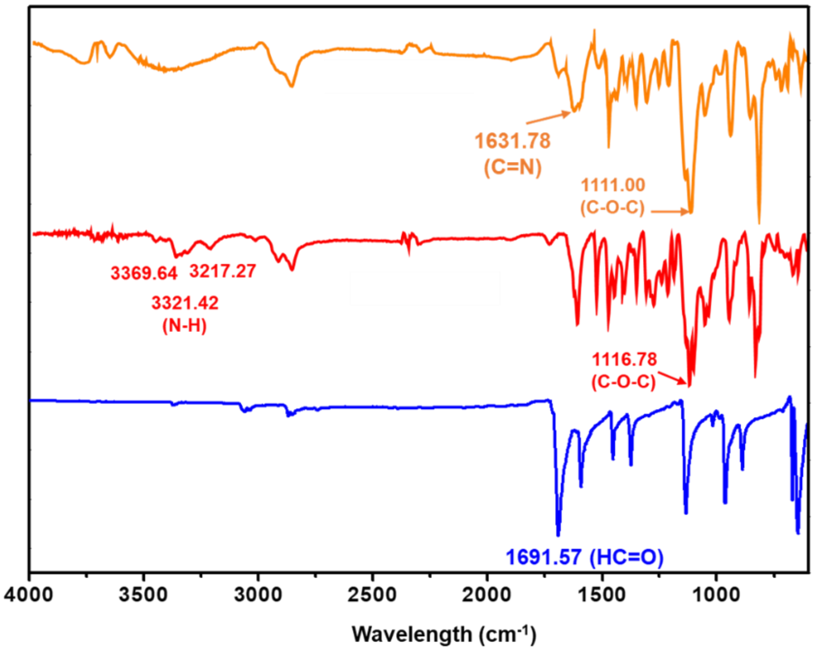

Figure S11. FT-IR spectra of **15C5-COF** (orange), **15C5-TPDA** (red) and 1,3,5-Triformylbenzene (blue).

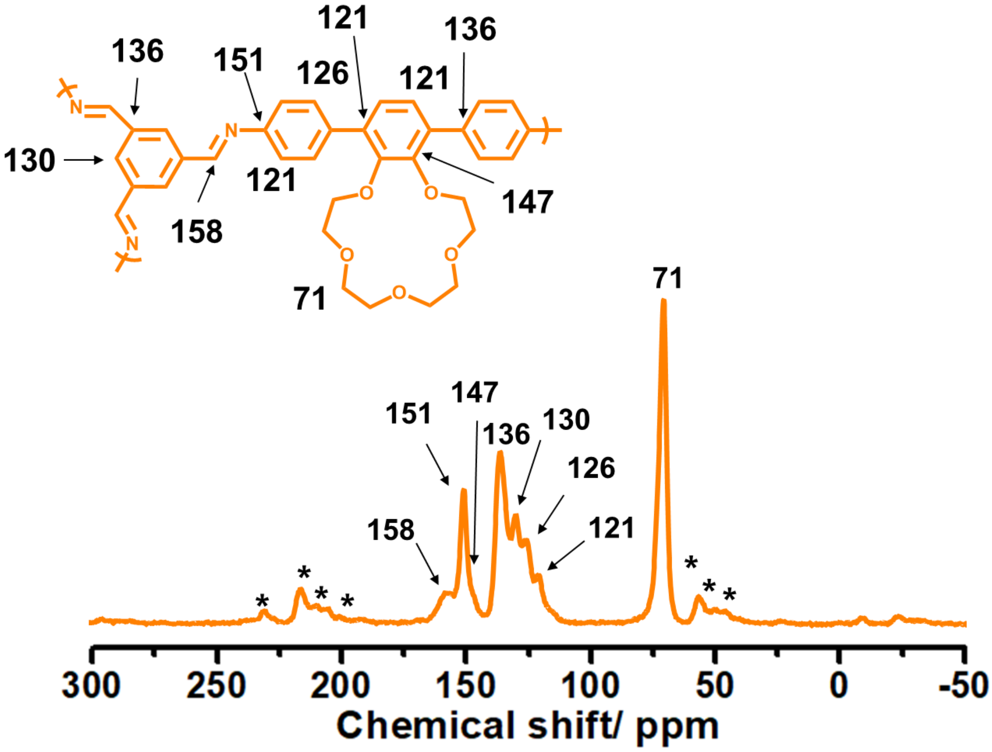

Figure S12. ^{13}C CP/MAS NMR spectrum of **15C5-COF**. The asterisks denote the spinning sidebands. The MAS spinning speed was 8 kHz.

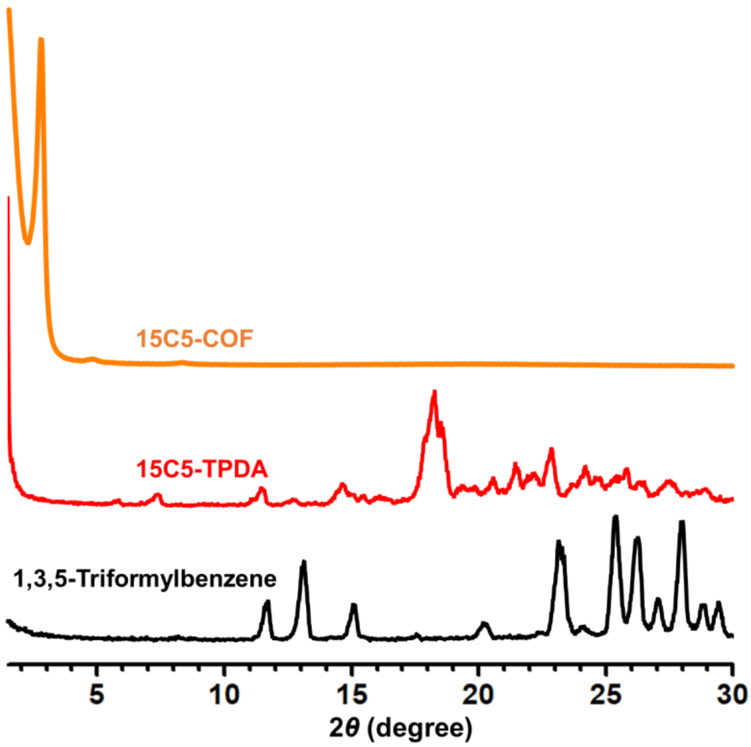

Figure S13. PXRD patterns of **15C5-COF** (orange), **15C5-TPDA** (red), and 1,3,5-Triformylbenzene (black).

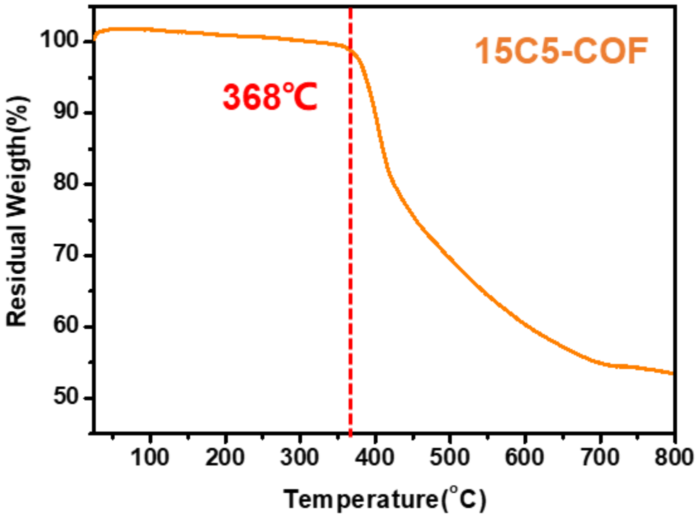

Figure S14.TGA data of **15C5-COF. 15C5-COF** is thermally stable up to 368 °C.

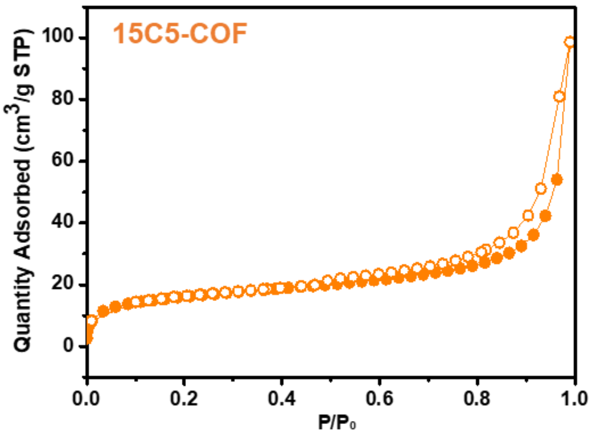

Figure S15. Nitrogen adsorption (filled symbols) and desorption (empty symbols) isotherms of **15C5-COF**. The profile showed a type-IV isotherm, which is characteristic for a mesoporous material

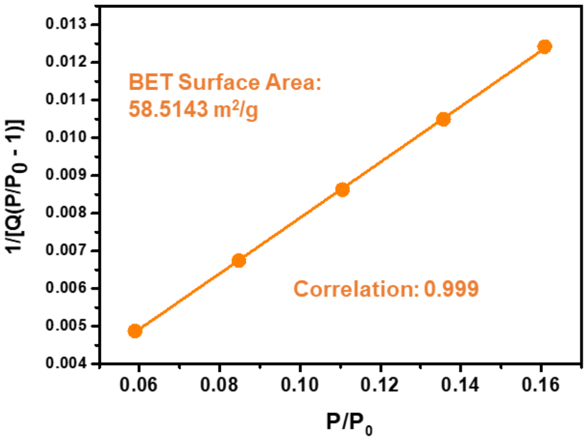

Figure S16. BET surface area plot for **15C5-COF** calculated from the absorption isotherm.

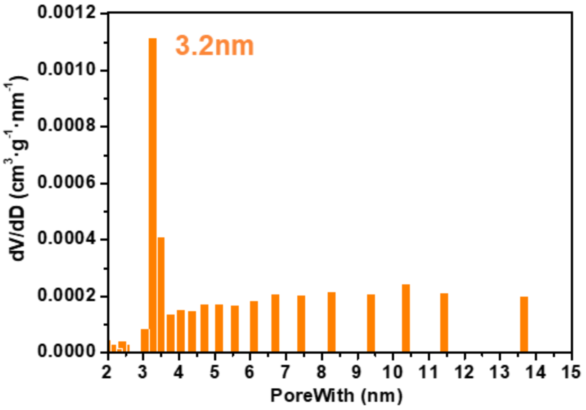

Figure S17. Pore size distribution of **15C5-COF** calculated by BJH method.

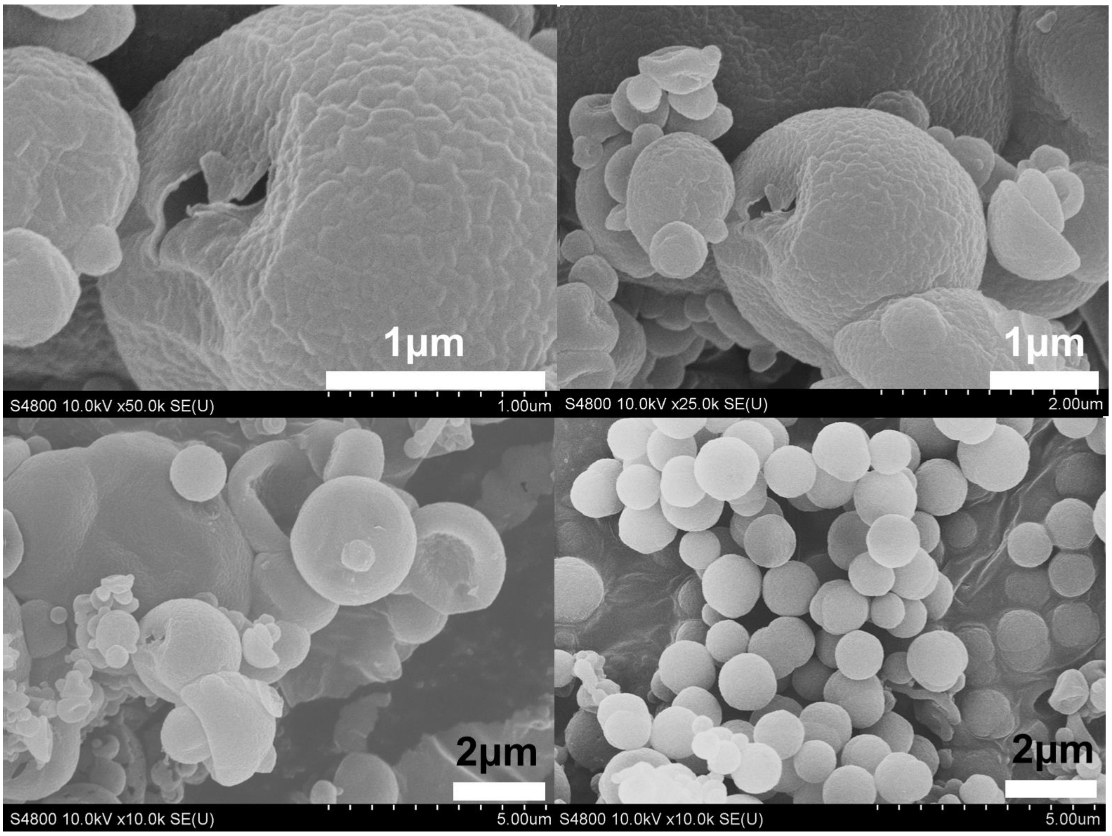

Figure S18. SEM image of **15C5-COF**. It can be seen that **15C5-COF** contain a hollow spherical shell structure.

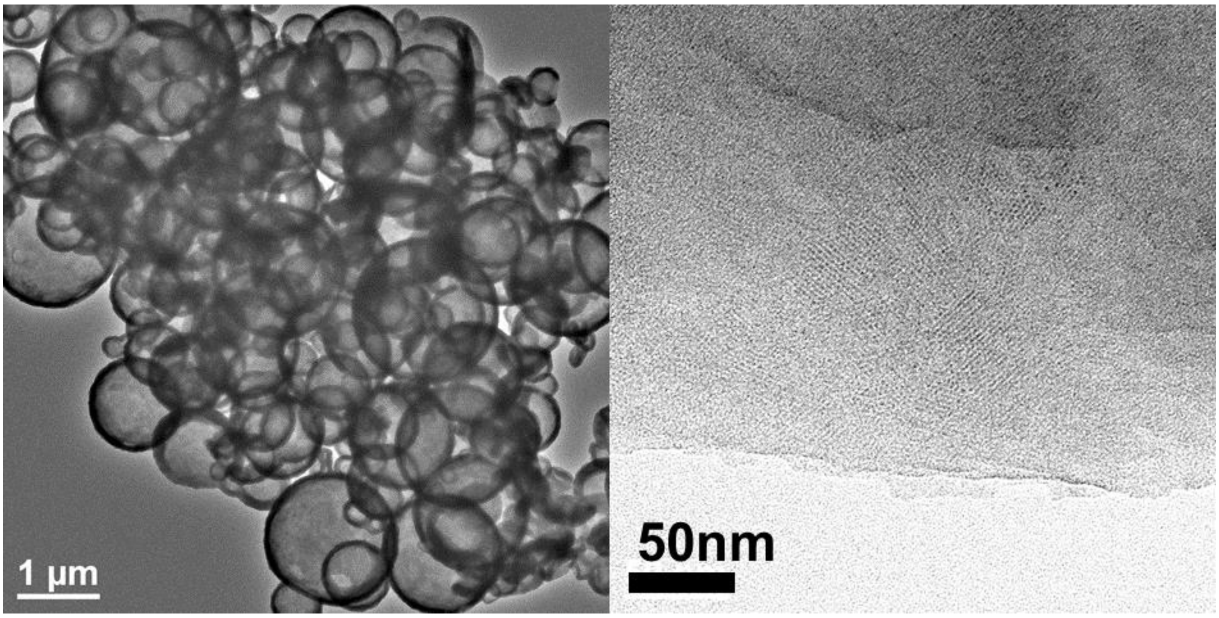

Figure S19. TEM image of **15C5-COF**.

3. Structural modeling and Powder X-Ray Diffraction analyses of 15C5-COF

The structural modeling process of **15C5-COF** was similar to that of **12C4-COF.** Pawley refinement of the experimental PXRD of **15C5-COF** was conducted to optimize the lattice parameters iteratively until the R_{wp} value converges, resulting in the cell parameters of a = b = 36.88841 ± 0.58938 Å, c = 4.54455 ± 0.07345 Å, α = β = 90° , and γ = 120° with R_{wp} = 2.27%, and R_{p} = 1.50%. A staggered arrangement (AB) for **15C5-COF** was also constructed with the space group P3, Comparison of the observed and the simulated PXRD patterns (Figure S20) suggested that the preferable structure of **15C5-COF** is the eclipsed arrangement (AA).

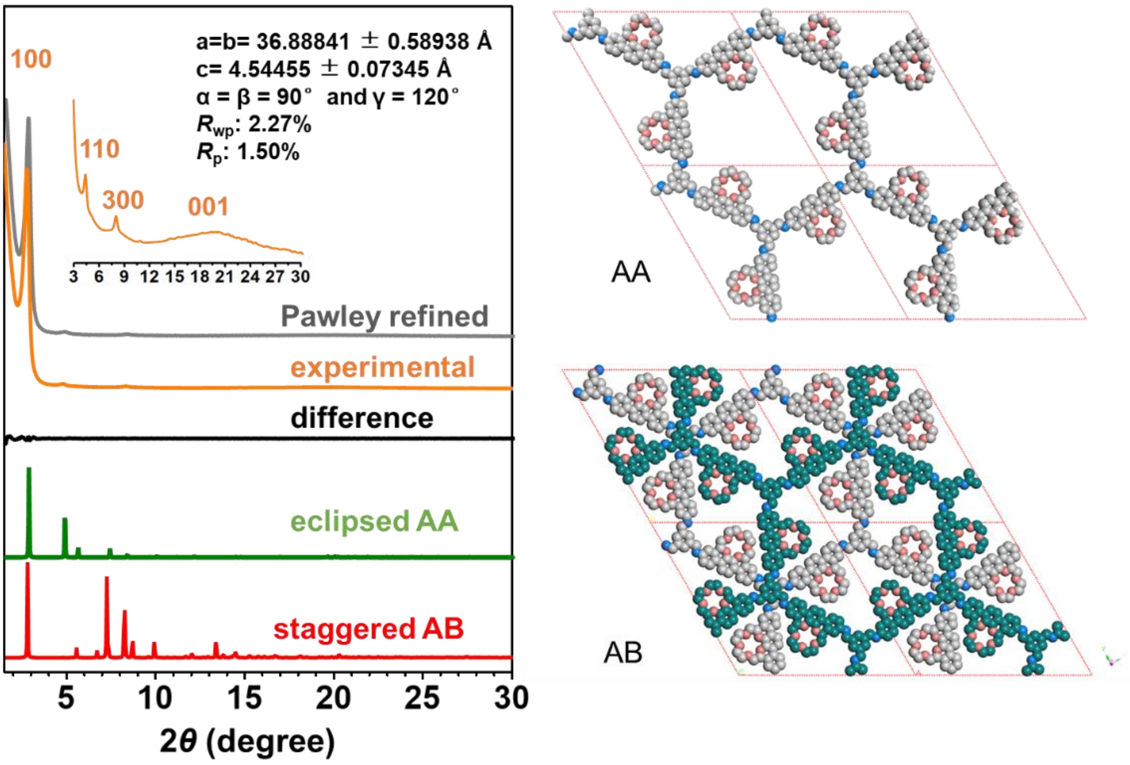

Figure S20. Left: PXRD patterns of **15C5-COF** observed (orange), Pawley refined patterns (light gray), difference plot between the observed and refined patterns (black) and calculated with the eclipsed AA (green) or staggered AB(red) stacking models. Right: Graphic views of AA (top) or AB (bottom) models. Comparison of the observed and the simulated PXRD patterns suggested that the preferable structure of **15C5-COF** is the eclipsed arrangement.

Table S2. Fractional atomic coordinates for the unit cell of **15C5-COF** with AA stacking

P3; a = b = 36.88841 ± 0.58938 Å; c = 4.54455 ± 0.07345 Å α = β = 90° and γ = 120°							
Atom	x	y	z	Atom	x	y	z
C1	1.29132	1.63493	0.72824	C36	1.62267	1.83562	1.02774
C2	1.30135	1.67696	0.7298	C37	1.64553	1.81581	1.09541
C3	1.26746	1.68698	0.76003	C38	1.68778	1.83896	1.16497
C4	1.57819	1.80929	0.93913	C39	1.70873	1.88286	1.17257
C5	1.75508	1.90555	1.21354	H40	1.25876	1.61049	0.73686
C6	1.77355	1.89117	1.41935	H41	1.23603	1.66177	0.80626
C7	1.81706	1.91103	1.44852	H42	1.7543	1.86481	1.56085
C8	1.84302	1.94616	1.27509	H43	1.83015	1.89956	1.61226
C9	1.82476	1.9611	1.07529	H44	1.84434	1.98816	0.94036
C10	1.78136	1.9405	1.03988	H45	1.76842	1.95191	0.87621
C11	1.54654	1.81274	1.08496	H46	1.55402	1.83398	1.26737
C12	1.5045	1.78625	1.01361	H47	1.48084	1.7888	1.13771
C13	1.49322	1.75494	0.79908	H48	1.5164	1.7261	0.49784
C14	1.52463	1.75057	0.65949	H49	1.5905	1.77393	0.61343
C15	1.56678	1.77781	0.72577	H50	1.9636	1.92232	1.39437
N16	1.4502	1.7249	0.73996	H51	1.89495	1.91804	1.42957
C17	1.95596	1.97649	1.39474	H52	1.72308	2.08525	1.29788
C18	1.97955	1.95623	1.39605	H53	1.75341	2.12132	1.00981
C19	1.90987	1.95128	1.38466	H54	1.79676	2.09148	0.95756
N20	1.8878	1.96793	1.30015	H55	1.79017	2.09127	1.34572
O21	1.64286	1.98623	0.87401	H56	1.70209	2.01333	1.35426
O22	1.62112	1.89986	0.93919	H57	1.74795	2.02861	1.58183
O23	1.70455	1.9474	1.11488	H58	1.75062	1.96761	1.44308
O24	1.75795	2.03327	1.12895	H59	1.69855	1.95205	1.56854
O25	1.71124	2.06154	0.8647	H60	1.60749	2.01656	0.78318
C26	1.73888	2.08821	1.08333	H61	1.64316	2.01885	0.50773
C27	1.77329	2.07705	1.1365	H62	1.67473	2.08678	0.73526
C28	1.732	2.01321	1.3739	H63	1.66266	2.06387	1.09788
C29	1.7216	1.96783	1.38924	H64	1.58089	1.93941	0.82031
C30	1.63863	2.01907	0.74839	H65	1.5928	1.96898	1.16129
C31	1.67257	2.06082	0.87229	H66	1.63764	1.93917	1.31475
C32	1.60476	1.95519	0.99614	H67	1.58333	1.90164	1.27697
C33	1.61215	1.92294	1.15233	H68	1.63071	1.78199	1.08871
C34	1.68544	1.90352	1.11962	H69	1.70454	1.82223	1.20125
C35	1.64244	1.87974	1.04363				

Section 5. Synthesis, characterization, and structural modeling of 18C6-COF

1. Synthesis of 18C6-COF

Scheme S4. Synthesis of **18C6-COF** by condensation of **18C6-TPDA** and 1,3,5-Triformylbenzene

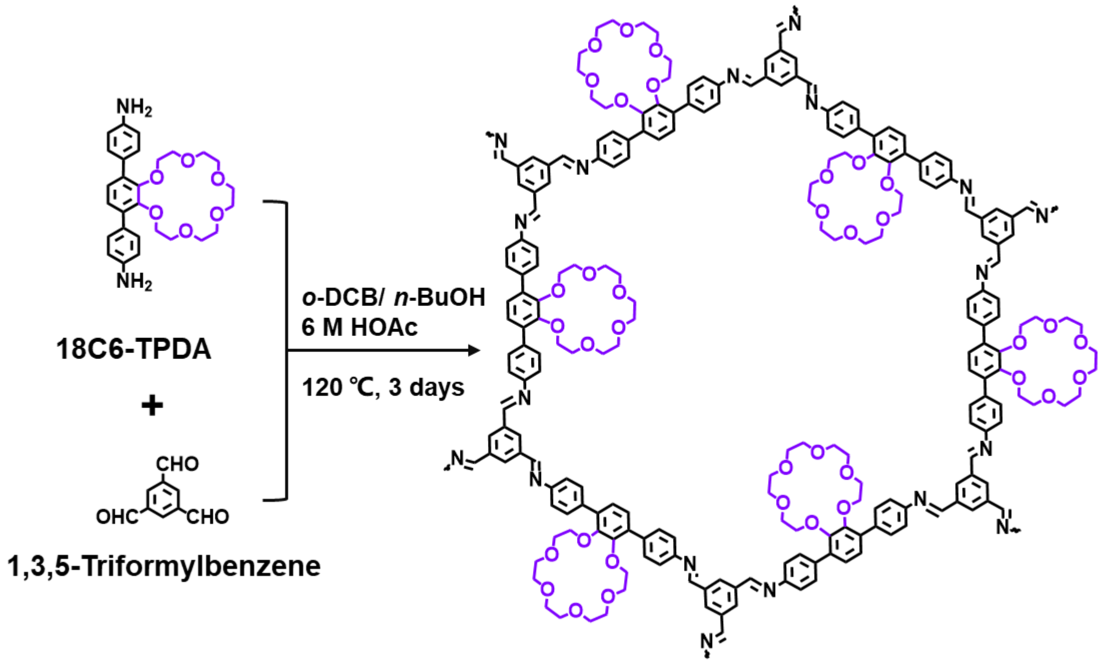

1,3,5-Triformylbenzene (19.46 mg, 0.12 mmol) and **18C6-TPDA** (89.0 mg, 0.18 mmol) were weighed into a 10 mL pressure ampoule (body length of 18 cm and neck length of 9 cm). To the mixture were added *o*-dichlorobenzene ***o*-DCB** (0.15 mL), *n*-BuOH (1.35 mL), and 6 M aqueous acetic acid (0.2mL). Then the ampoule was flash frozen in a liquid nitrogen bath, evacuated to an internal pressure of 0.1 Pa and flame sealed, reducing the total length by *ca.* 10 cm. After warming to room temperature, the sealed ampoule was placed in an oven at 120 °C and left undisturbed for 3 days, yielding a yellow solid. The ampoule was opened when the mixture was still warm (over 40 °C) and the solid was transferred into a 10mL centrifuge-tube, separated by centrifugation, washed with DMF (3 × 8 mL), THF (3 × 8 mL) and acetone (3 × 8 mL). The resulting solid was further dried under vacuum at 100 ° C for 12 hours, to yield **18C6-COF** as a yellow powder (86.2 mg, 84.5% yield). Further purification of **18C6-COF** was carried out by Soxhlet extraction in THF for 12 h. Anal. Cald. for $(C_{17}H_{17}NO_3)_n$: C 72.08; H 6.00; N 4.95. Found: C 67.69; H 6.04; N 4.18.

2. Characterization of 18C6-COF

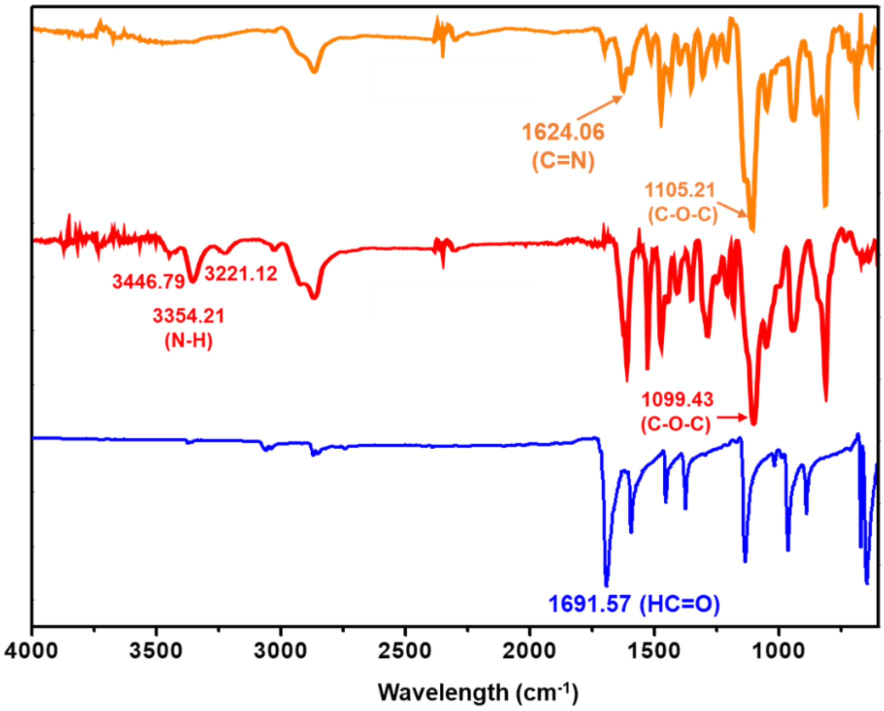

Figure S21. FT-IR spectra of **18C6-COF** (orange), **18C6-TPDA** (red) and 1,3,5-Triformylbenzene (blue).

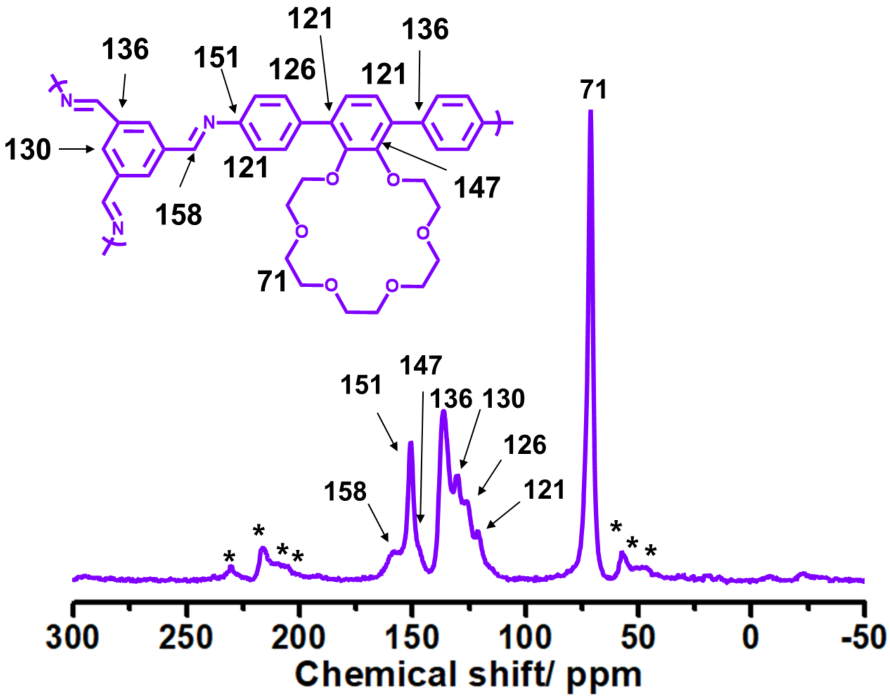

Figure S22. ^{13}C CP/MAS NMR spectrum of **18C6-COF**. The asterisks denote the spinning sidebands. The MAS spinning speed was 8 kHz.

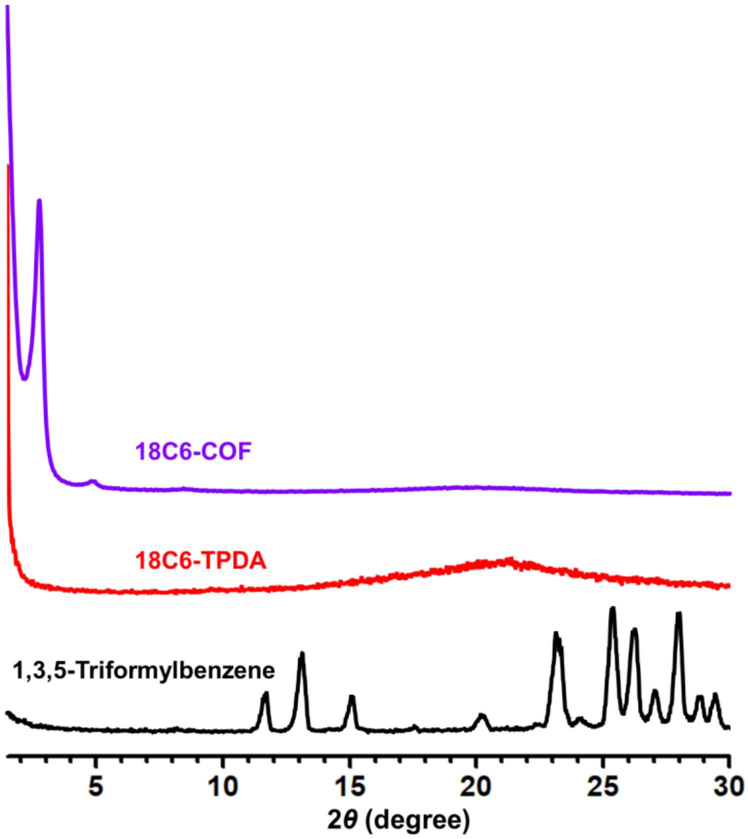

Figure S23. PXRD patterns of **18C6-COF** (purple), **18C6-TPDA** (red), and 1,3,5-Triformylbenzene (black).

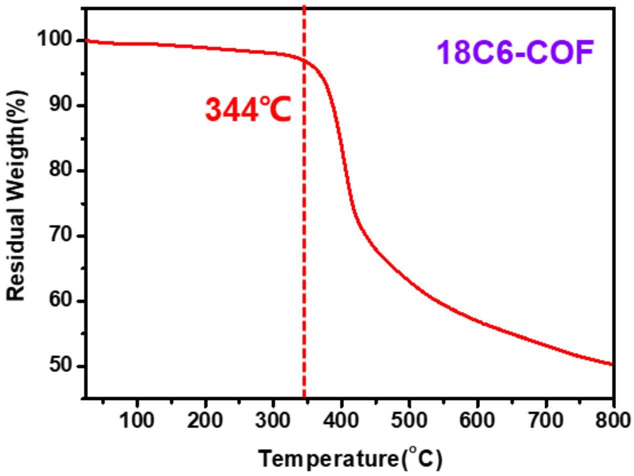

Figure S24.TGA data of **18C6-COF. 18C6-COF** is thermally stable up to 344 °C.

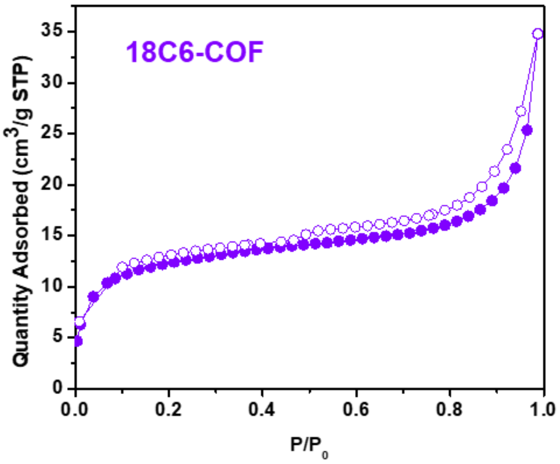

Figure S25. Nitrogen adsorption (filled symbols) and desorption (empty symbols) isotherms of **18C6-COF**. The profile showed a type-IV isotherm, which is characteristic for a mesoporous material

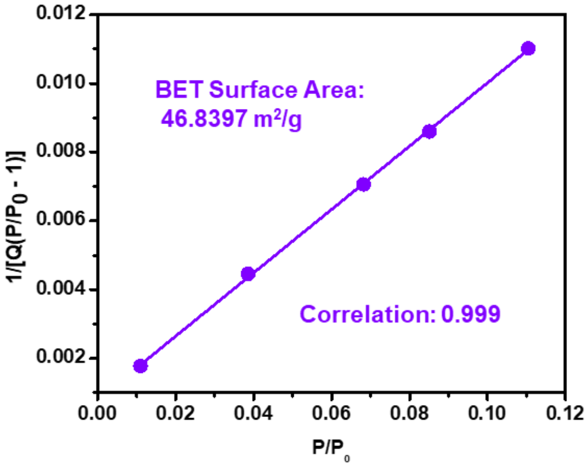

Figure S26. BET surface area plot for **18C6-COF** calculated from the absorption isotherm.

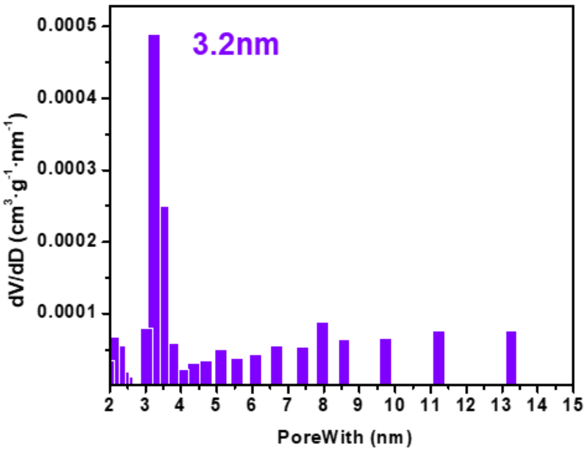

Figure S27. Pore size distribution of **18C6-COF** calculated by BJH method.

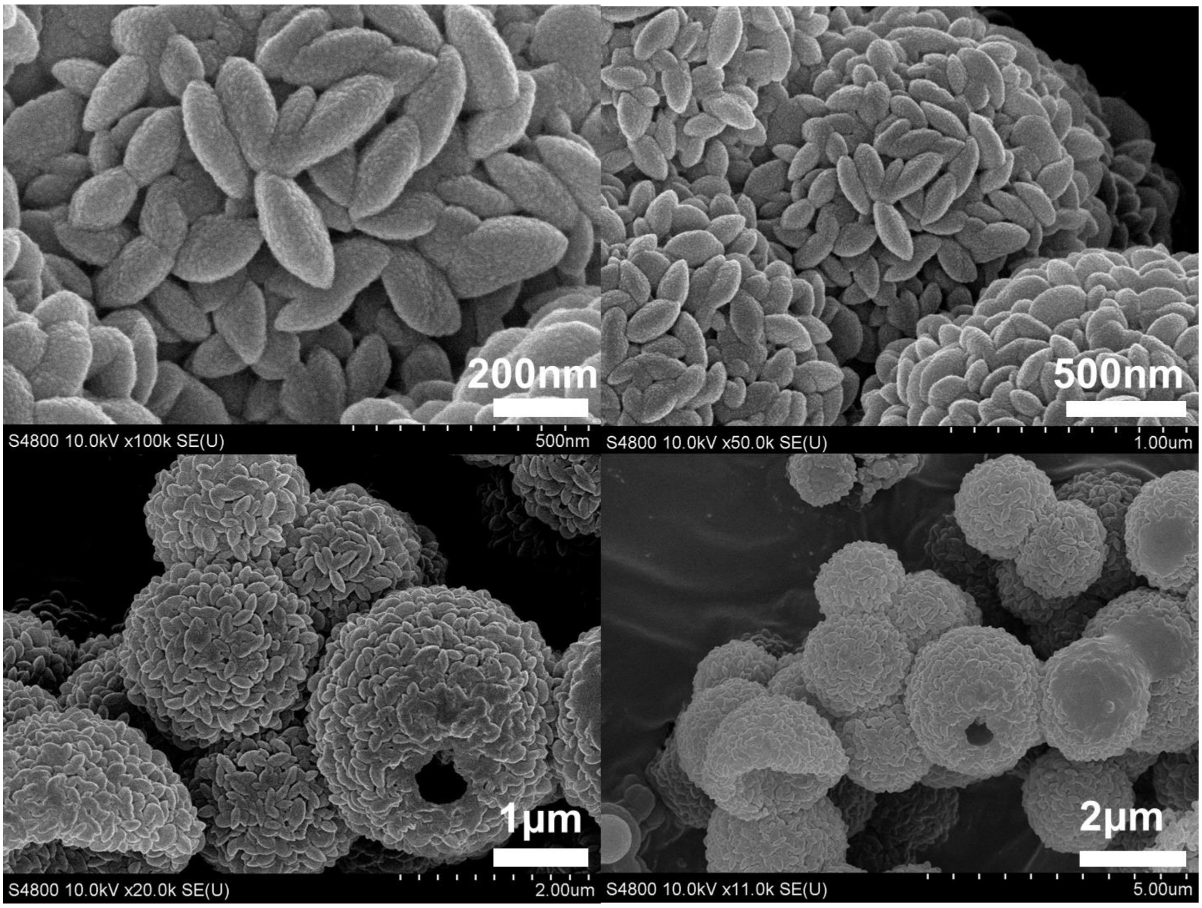

Figure S28. SEM image of **18C6-COF.** The image showed that the spherical shell of **18C6-COF** obviously consists of rice-shaped particles

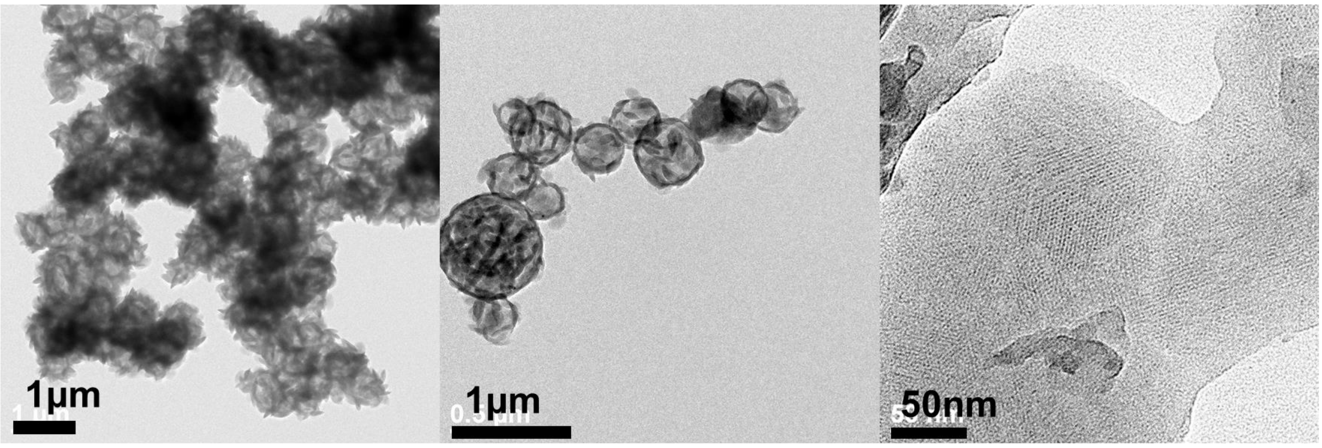

Figure S29. TEM image of **18C6-COF**

3. Structural modeling and Powder X-Ray Diffraction analyses of 18C6-COF

The structural modeling process of **18C6-COF** was similar to that of **12C4-COF.** Pawley refinement of the experimental PXRD of **18C6-COF** was conducted to optimize the lattice parameters iteratively until the R_{wp} value converges, resulting in the cell parameters of a = b = 36.76938 ± 0.69602 Å, c = 4.24257 ± 0.08145 Å, α = β = 90° , and γ = 120° with R_{wp} = 3.35%, and R_p = 2.63%. A staggered arrangement (AB) for **18C6-COF** was also constructed with the space group P3, Comparison of the observed and the simulated PXRD patterns (Figure S30) suggested that the preferable structure of **18C6-COF** is the eclipsed arrangement (AA).

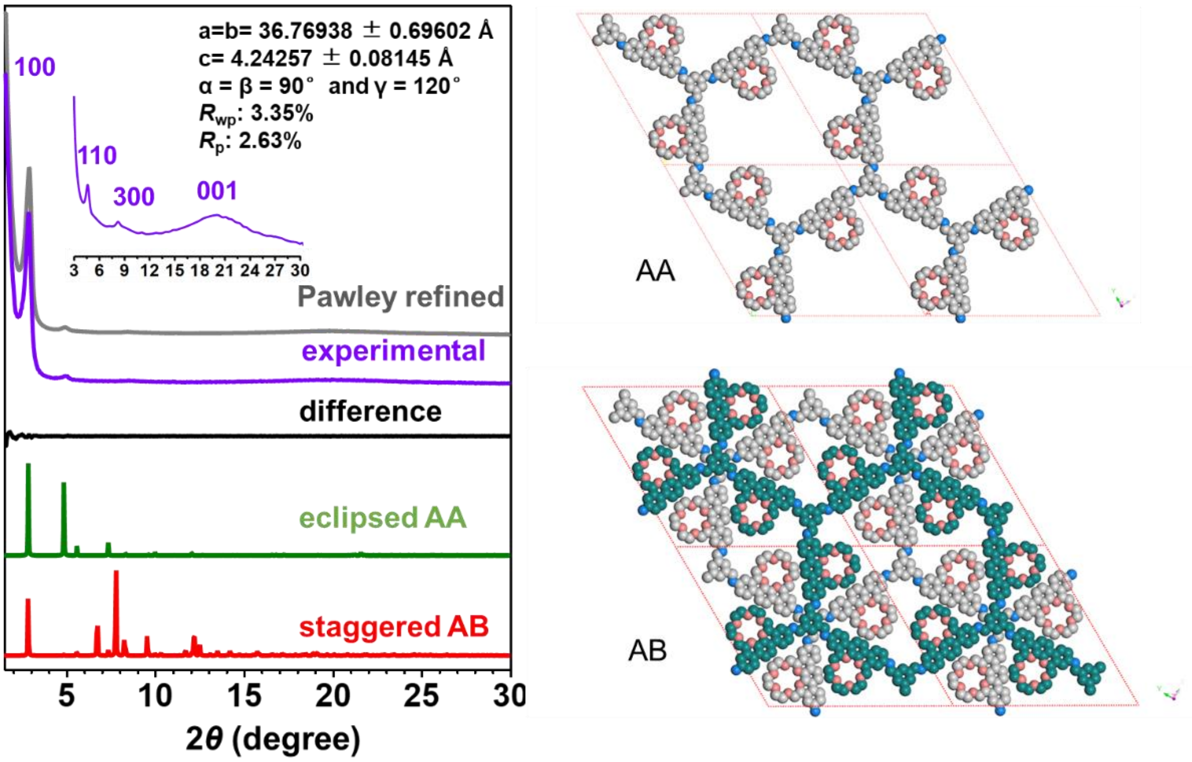

Figure S30. Left: PXRD patterns of **18C6-COF** observed (purple), Pawley refined patterns (light gray), difference plot between the observed and refined patterns (black) and calculated with the eclipsed AA (green) or staggered AB(red) stacking models. Right: Graphic views of AA (top) or AB (bottom) models. Comparison of the observed and the simulated PXRD patterns suggested that the preferable structure of **18C6-COF** is the eclipsed arrangement.

Table S3. Fractional atomic coordinates for the unit cell of **18C6-COF** with AA stacking

P3; a = b = 36.76938 ± 0.69602 Å; c = 4.24257 ± 0.08145 Å
α = β = 90° and γ = 120°

Atom	x	y	z	Atom	x	y	z
O1	0.36596	0.30439	0.90597	N39	1.36641	0.5875	1.3881
O2	0.43413	0.38907	1.02261	C40	1.35743	0.64664	1.50442
O3	0.39254	0.4317	1.24924	C41	1.37721	0.69058	1.50683
O4	0.28586	0.35127	1.09036	C42	1.38323	0.62638	1.47809
O5	0.22012	0.27616	0.91994	H43	0.22998	0.19541	1.17847
O6	0.27695	0.24252	0.88627	H44	0.21378	0.20426	0.80598
C7	0.23541	0.22052	1.00584	H45	0.19238	0.23175	1.27454
C8	0.22328	0.25072	1.15534	H46	0.24735	0.2702	1.33432
C9	0.21125	0.30603	1.05708	H47	0.20356	0.3012	1.31381
C10	0.24819	0.35027	1.00734	H48	0.18325	0.30363	0.93771
C11	0.34906	0.26098	0.96004	H49	0.24953	0.35883	0.75453
C12	0.30567	0.24269	1.10869	H50	0.24254	0.37228	1.15253
C13	0.40657	0.32116	0.77572	H51	0.36929	0.25543	1.12557
C14	0.42567	0.36819	0.72558	H52	0.34618	0.244	0.73581
C15	0.43254	0.4536	1.10824	H53	0.29619	0.21021	1.1872
C16	0.45452	0.43302	1.00668	H54	0.30791	0.2621	1.31648
C17	0.31801	0.39291	1.14865	H55	0.40503	0.30655	0.54289
C18	0.36036	0.39622	1.08566	H56	0.42769	0.316	0.93483
C19	0.4979	0.45729	0.9244	H57	0.45486	0.37949	0.58864
C20	0.51723	0.50133	0.93338	H58	0.40366	0.37408	0.58749
C21	0.49504	0.52114	1.01888	H59	0.31631	0.40065	1.39951
C22	0.45291	0.49781	1.10785	H60	0.31551	0.41631	0.99646
C23	0.67743	0.3756	0.66625	H61	0.35927	0.36729	1.17375
C24	0.63493	0.34411	0.6676	H62	0.3658	0.39897	0.8274
C25	0.60125	0.35464	0.69385	H63	0.55031	0.52105	0.88244
C26	0.52484	0.43846	0.84711	H64	0.51112	0.55514	1.0177
C27	0.51944	0.40207	0.9997	H65	0.68594	0.40838	0.67378
C28	0.54602	0.38608	0.93599	H66	0.56936	0.32952	0.73411
C29	0.57967	0.40691	0.72511	H67	0.4958	0.38652	1.17777
C30	0.58596	0.44358	0.57787	H68	0.54146	0.35871	1.06471
C31	0.55834	0.45863	0.63157	H69	0.61189	0.46009	0.4156
N32	0.60958	0.39331	0.67383	H70	0.56338	0.48616	0.50266
C33	1.43017	0.52021	1.19464	H71	1.47924	0.56545	1.49907
C34	1.44876	0.55531	1.39511	H72	1.44304	0.60392	1.62426
C35	1.42813	0.57757	1.46435	H73	1.33928	0.51991	1.03266
C36	1.38846	0.56509	1.33261	H74	1.37637	0.48211	0.8989
C37	1.36965	0.5297	1.13758	H75	1.41119	0.70898	1.50092
C38	1.39052	0.50781	1.06519	H76	1.41667	0.64553	1.5076

Section 6. Ion adsorption test of CE-COFs

50 mg **CE-COF** and 20 mL aqueous solution containing LiI, NaI or KI (10 mmol/L) were mixed and stirred in a 25 mL glass vial (3×3 groups independently) at 25 ℃. The mixture was centrifuged at 3000 rpm for 5 minutes to present a supernatant liquid every 1 hour, and the ion concentration in the supernatant was determined by an inductively coupled plasma optical emission spectrometer (ICP-OES, Agilent Technology 5100). The ion adsorbing capacity (Q, mmol/g) was calculated by the following equation.[3] It was found that adsorption equilibrium was reached in about 4 hours.

$$Q = \frac{(C_0 - C_e)V}{m}$$

where V is the volume (mL) of aqueous solution; C_0 and C_e are the ion concentration (mmol/L) in the aqueous phase before and after adsorption, respectively. m is the mass (g) of **CE-COF** powder.

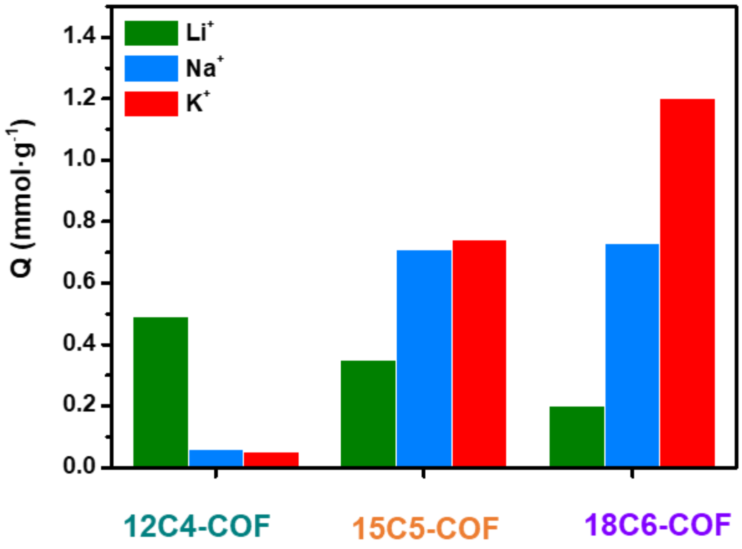

Figure S34. Bar chart of overall adsorption of alkali metal ions by crown ether

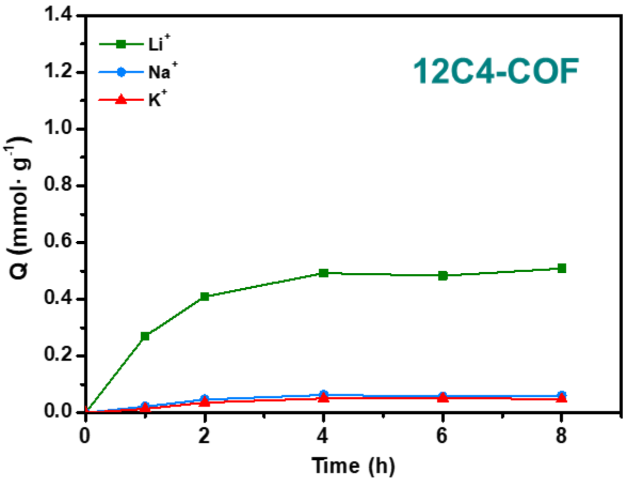

Figure S31. Adsorption kinetics of ions on **12C4-COF**. The adsorption capacity of Li⁺, Na⁺ and K⁺ are 0.5, 0.06 and 0.05 mmol/g, respectively.

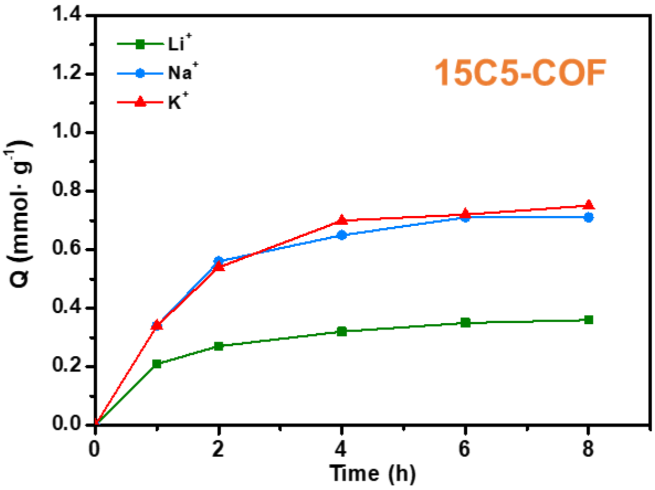

Figure S32. Adsorption kinetics of ions on **15C5-COF**. The adsorption capacity of Li⁺, Na⁺ and K⁺ are 0.35, 0.71 and 0.74 mmol/g, respectively.

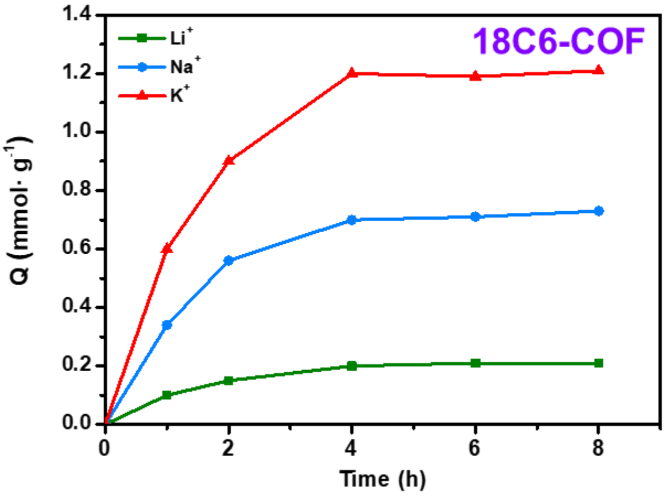

Figure S33. Adsorption kinetics of ions on **18C6-COF**. The adsorption capacity of Li⁺, Na⁺ and K⁺ are 0.20, 0.73 and 1.20 mmol/g, respectively.

Section 7. Catalytic activity test of 18C6-COF for iodination of 1-bromooctane

1. General experimental procedure

$$\text{n-}C_8H_{17}Br \xrightarrow[\text{THF. 70℃, 10h}]{\text{KI (5 equiv.), 5 mol\% 18C6-COF}} \text{n-}C_8H_{17}I$$

A mixture of 1-bromooctane (48.0 mg, 0.25 mmol), potassium iodide (208.0 mg, 1.25 mmol), THF (2.0 mL) and the **18C6-COF** (7.1 mg, 5 mol %) was refluxed at 70 ℃ for 10 h. After diluting the solution sample (10.0 μL) with dichloromethane (2.0 mL), it was analyzed by gas chromatograph-mass spectrometer GC-MS to determine the conversion to product (keep at 50 ℃ for 1min, followed by 20 ℃ /min ramp to 115 ℃ for 3 min, and followed by 45 ℃ /min ramp to 195 ℃, held for 1 min. Injector: 300 ℃, Interface Temperature: 300 ℃. Rt. 7.57 min (1-bromooctane), 8.73 min (1-iodooctane).

Solvent screening, orthogonal experiments, and catalyst comparison tests were all performed in the similar procedure above.

To get the dynamic curve of the reaction, the reaction was monitored by taking samples (10 μL) every two-hour. The sample was diluted with 2 mL dichloromethane for GC-MS detection. Taking the yield of 1-iodooctane as the ordinate, reaction time as the abscissa, and a reaction rate curve was obtained.

Table S4. The rate of formation of 1-iodooctane.

	Time (h)	0	2	4	6	8	10
Yield[a] (%)	No Catalyst	0	6.36	13.29	17.44	21.91	25.12
	18C6-TPDA	0	18.2	28.1	35.42	41.43	46.16
	18C6-COF	0	55.66	77.82	88.93	94.89	96.46

[a] raw data read from GC, and used for depicting the dynamic curve and for the calculation of rate constant.

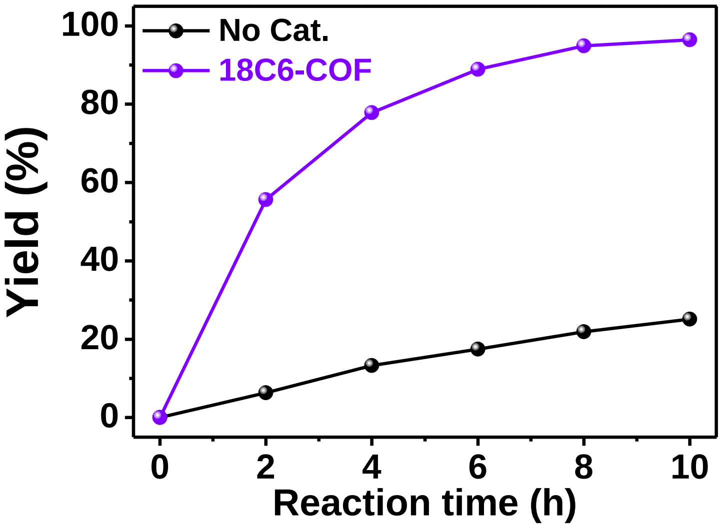

Figure S35. The kinetics of formation of 1-iodooctane

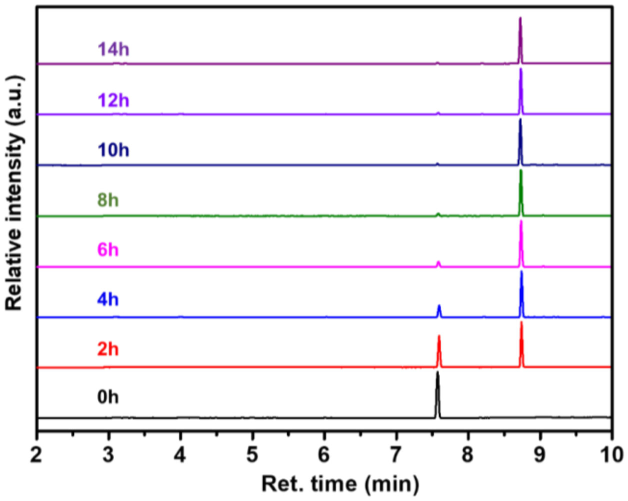

Figure S36. Gas chromatography (GC) analysis of the reaction solution, indicating the progress of the 1-bromooctane (7.57 min) to 1-iodooctane (8.73 min).

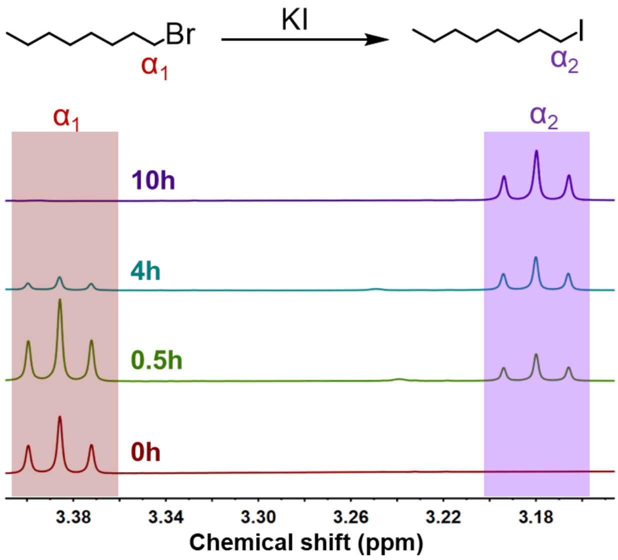

Figure S37. Partial ^{1}H NMR spectrum of the conversion process, the α-H were highlighted.

2. Calculation of rate constant

Due to the large excess of KI, the KI concentration[B] in the solution is always saturated, which is considered to be constant, and the COF is in a solid phase. The reaction rate is only related to the concentration of 1-bromooctane [A]. Thus, it can be regarded as a first order reaction If the product formation rate is set to x, the concentration of the 1-iodooctane [C] is proportional to x, then, [A] is proportional to (1-x) and the following simple calculations are performed:

Taking the reaction time t as the abscissa and -ln(1-x) as the ordinate, the fit yields a straight line, as shown in the following figure, where the slope is the apparent rate constant k' of the reaction (k_0'=0.029 s^{-1} , k_1'=0.341 s^{-1}) with a good correlation 0.988 and 0.990, respectively.

$$\underset{B}{\mathrm{KI}} + \underset{A}{n\text{-}C_8H_{17}Br} \longrightarrow \underset{C}{n\text{-}C_8H_{17}I}$$

$$\frac{\mathrm{d}[C]}{\mathrm{d}t} = k[A][B]$$

$$\frac{\mathrm{d}[C]}{\mathrm{d}t} = k' [A]$$

$$\frac{d[C]}{[A]} = k' d t$$

$$\frac{dx}{1-x} = k' d t$$

$$-\ln(1\text{-}x) = k''t$$

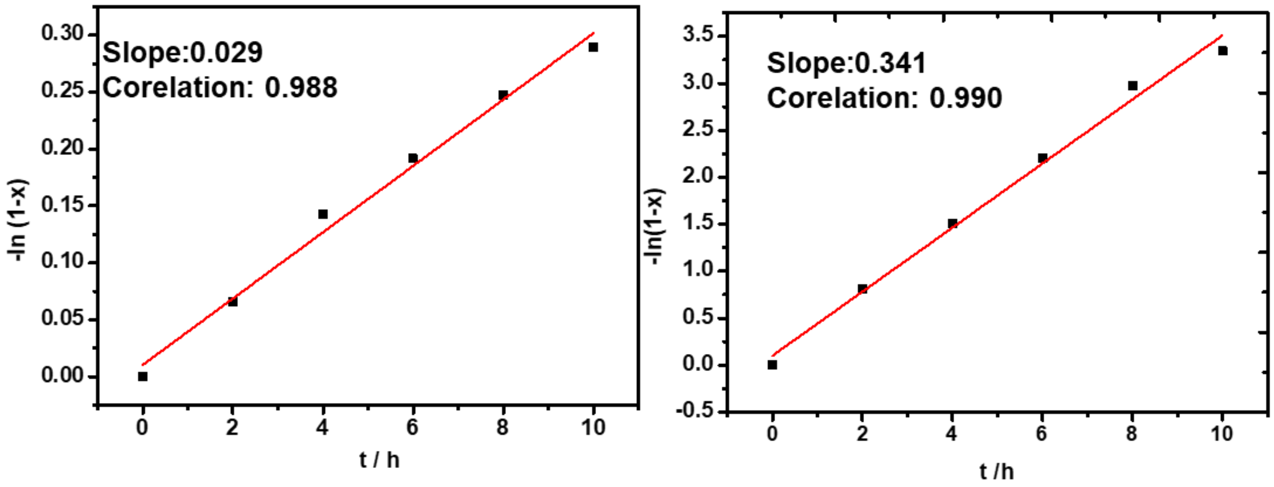

Figure S38.The linear fitting between -ln(1-x) and reaction time in absence (the left)/ presence (the right) of **18C6-COF**, x refers to the yield of 1-iodooctane.

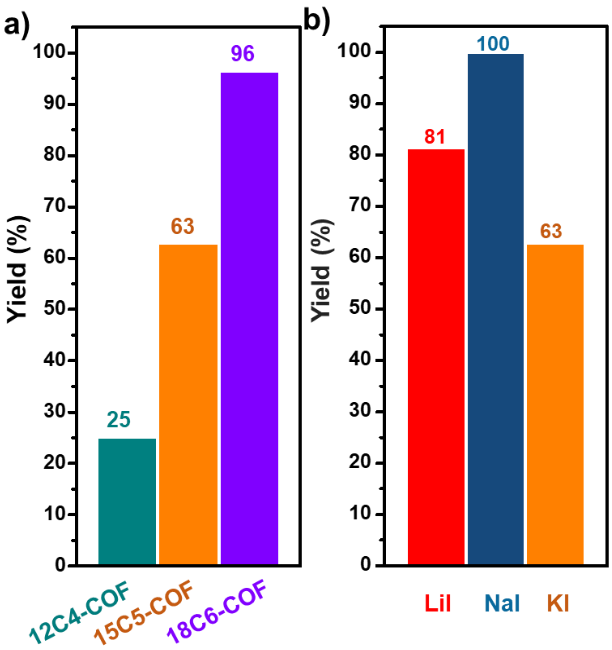

Figure S39. The orthogonal tests by using KI with different crown ethers as catalysts (a)﹐and (b) by using **15C5-COF** with LiI, NaI and KI as the substrates in the iodination of 1-bromooctane.

3. Recycle test of 18C6-COF for iodination of 1-bromooctane

The recyclability of **18C6-COF** was tested for the iodination of 1-bromooctane under the same condition except that all the substrate and solvent is magnified by 4 times. After each cycle, **18C6-COF** was recovered by centrifugation, washed with CH_2Cl_2 (1 × 10 mL), H_2O (2 × 10 mL), THF (1 × 10 mL), and Acetone (1 × 6 mL). The resulting powder was dried at 70 ℃, and then used for the next cycle. The catalytic results were summarized in Figure S40.

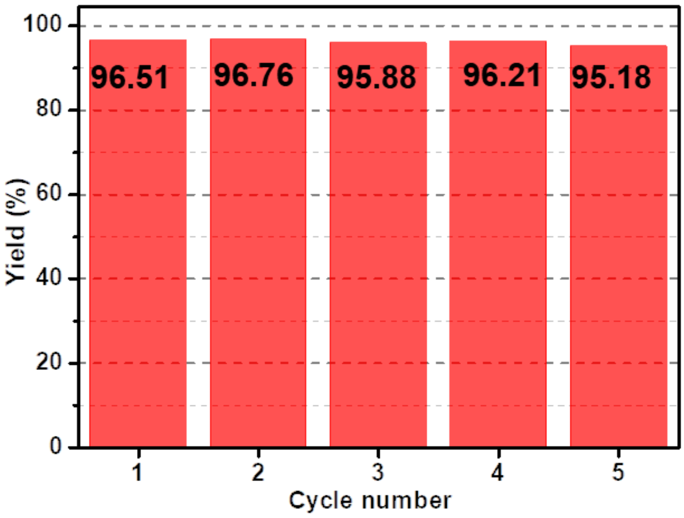

Figure S40. Recycle test of **18C6-COF** for five times. Conditions: 1-bromooctane (193 mg, 1.0 mmol), potassium iodide (840 mg, 5.0 mmol), THF (8.0 mL) and the **18C6-COF** (28.4 mg, 5 mol %) was refluxed at 70 ℃ for 10 h. Yield determined by GC.

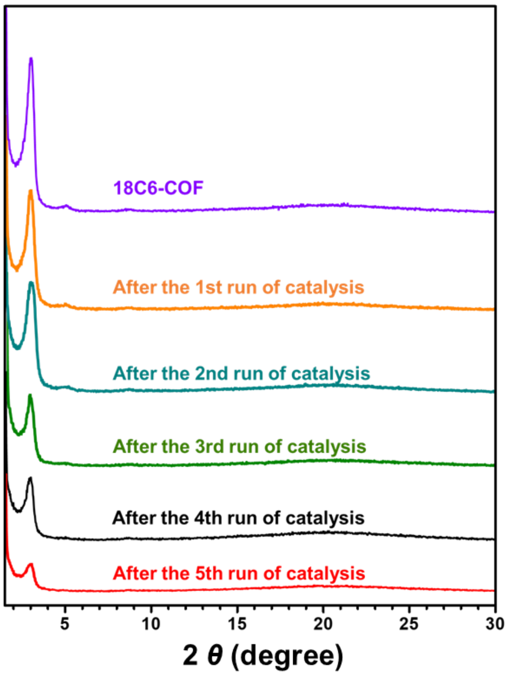

Figure S41. PXRD patterns of **18C6-COF** through the 5 recycle tests.

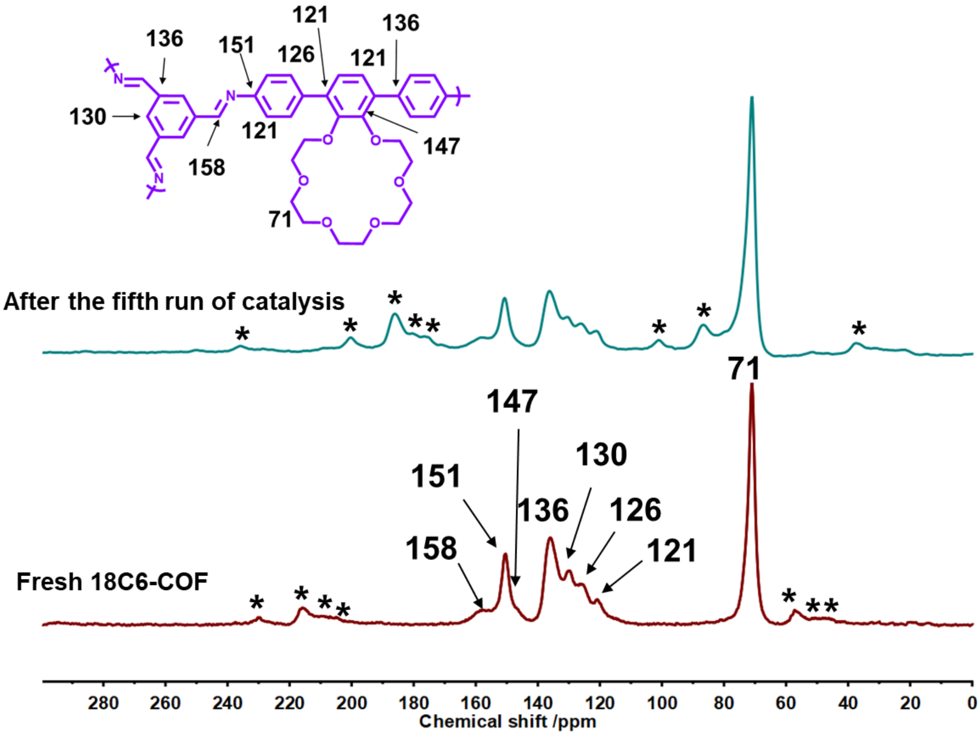

Figure S42. ^{13}C CP/MAS NMR spectrum of the fresh **18C6-COF** (bottom) and that after the fifth run of catalysis. After 5 cycles of catalysis, the signal peak did not disappear compared to fresh COF, meaning that the chemical structure of the material was maintained. Asterisks denote the spinning sidebands. Noting: The position of the spinning sidebands is different due to the use of different of MAS spinning speed of the samples (the top spectrum: 5 kHz, the bottom spectrum: 8 kHz).

Section 8. Catalytic activity test of 18C6-COF in Different Nucleophilic Substitution

1. General experimental procedure:

$$\text{R-X} + \text{Nu}^- \xrightarrow[\text{Solv. reflux}]{\text{10\% mol 18C6-COF}} \text{RNu} + \text{X}^-$$

A mixture of halohydrocarbon (R-X, 0.25 mmol), nucleophile (Nu^-, 1.25 mmol) and **18C6-COF** (14.2 mg, 10 mol %) were stirred in 2 mL CH_3CN (DMF in entry 12) and refluxed at 85 ℃ (100 ℃ in entry 12) for proper time vary from 1 to 24 hours. Noting: There are some differences in in entry 5. The mixture of benzoic acid (1.25 mmol), potassium hydroxide (1.5 mmol) stirred in H_2O (1.5 mL) for 10 mins, and then benzyl bromide (0.25mmol), 18C6-COF (14.2 mg, 10 mol %) in 0.5mL nitrobenzene was added and refluxed for 10 hours. After diluting the solution sample (10 μL) with dichloromethane (2 mL), it was analyzed by gas chromatograph-mass spectrometer GC-MS to determine the conversion to product (keep at 50 ℃ for 1min, followed by 20 ℃ /min ramp to 115 ℃ for 3 min, and followed by 45 ℃ /min ramp to 200 ℃, held for 3 min, further warm up to 240 ℃ by 10 ℃ /min, held for 1min. Injector: 300 ℃, Interface Temperature: 300 ℃. The detailed information of retention time (Rt.) are in the Table S5.

Table S5. The detailed information of different nucleophilic substitution catalysed by **18C6-COF**

$$\text{R-X} + \text{Nu}^- \xrightarrow[\text{Solv. reflux}]{\text{10\% mol 18C6-COF}} \text{RNu} + \text{X}^-$$

Entry	R-X	Rt. (min)	Nu^-	Product	Rt. (min)	Solvent	T(℃)	Time (h)	Yield (%)	Controlled Yield (%)
1	C_4H_9Br	1.6	CH_3COOK	$CH_3COOC_4H_9$	8.9	CH_3CN	85	5	85	27
2	$C_8H_{17}Br$	7.2	CH_3COOK	$CH_3COOC_8H_{17}$	8.0	CH_3CN	85	5	91	26
3	$PhCH_2Br$	6.8	CH_3COOK	CH_3COOCH_2Ph	7.4	CH_3CN	85	5	99	34
4	$PhCH_2Cl$	5.2	CH_3COOK	CH_3COOCH_2Ph	7.4	CH_3CN	85	5	81	13
5	$PhCH_2Br$	6.8	PhCOOK	$PhCOOCH_2Ph$	13.6	Nitrobenzene/H_2O	100	10	96	25
6	$PhCH_2Br$	6.8	KSCN	$PhCH_2SCN$	10.0	CH_3CN	85	1	99	31
7	$PhCH_2Br$	6.8	PhOK	$PhCH_2OPh$	11.6	CH_3CN	85	5	94	23
8	$PhCH_2Br$	6.8	NaN_3	$PhCH_2N_3$	6.6	CH_3CN	85	5	97	36
9	$PhCH_2Br$	6.8	KCN	$PhCH_2CN$	7.1	CH_3CN	85	10	82	N.D.
10	$PhCH_2Br$	6.8	KF	$PhCH_2F$	4.7	CH_3CN	85	10	84	N.D.
11	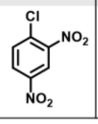	12.7	KF		10.9	CH_3CN	85	24	47	N.D.
12						DMF	100	10	86	32

2.Chemical stability test of 18C6-COF in hot solvent

According to the conditions of different nucleophilic substitution mentioned in the manuscript, 20 mg **18C6-COF** was soaked and dispersed in 2 mL solvent at a high temperature for 24 hours, including CH_3CN at 85 ℃, DMF at 100 ℃, water at 100 ℃ , Nitrobenzene at 100 ℃ and Water/nitrobenzene mixture at 100 ℃. After the soaking, the COF was filtered and washed by THF and acetone. The resulting powder was dried at 70 ℃; The dried COF was weighed to calculated the residual weight percentage, and the PXRD of the COF was tested to evaluate the remained crystalline structure. The residual weight and PXRD results were summarized in Figure S43.

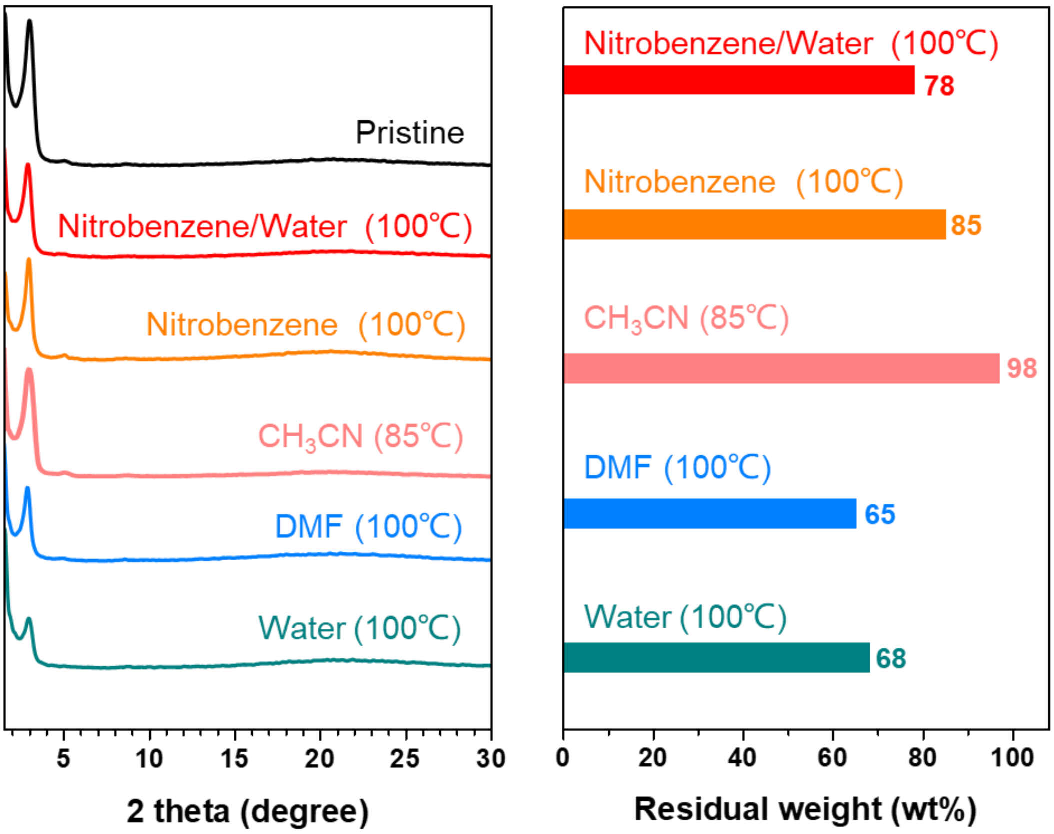

\

Figure S43. The PXRD (left) and residual weight (right) of **18C6-COF** after soaking in different solvents at a high temperature for 24 hours.

3.Recycle test of 18C6-COF in the esterification of benzoic acid and benzyl bromide

The recyclability of **18C6-COF** in the esterification of benzoic acid and benzyl bromide was investigated in water/nitrobenzene mixture. The initial conditions were: 2.5 mmol PhCOOH + 3.0 mmol KOH in 3.0 mL H_2O and 0.5 mmol $PhCH_2Br$ in 1.0 mL nitrobenzene, 10 mol% **18C6-COF** 28 mg, at 100 ℃, for 10 hours. After each cycle, **18C6-COF** was recovered by centrifugation, washed with H_2O (2 × 10 mL), THF (1 × 10 mL) and Acetone (1 × 6 mL). The resulting powder was dried at 70 ℃, and then used for the next cycle. The amount of substrate and solvent in the cycled experiments was calculated based on the mass of the recovered **18C6-COF** (**18C6-COF** accounts for 10 mol%). The catalytic results were summarized in Figure S44. (the final residual weight percentages was 72% after the third run of catalysis).

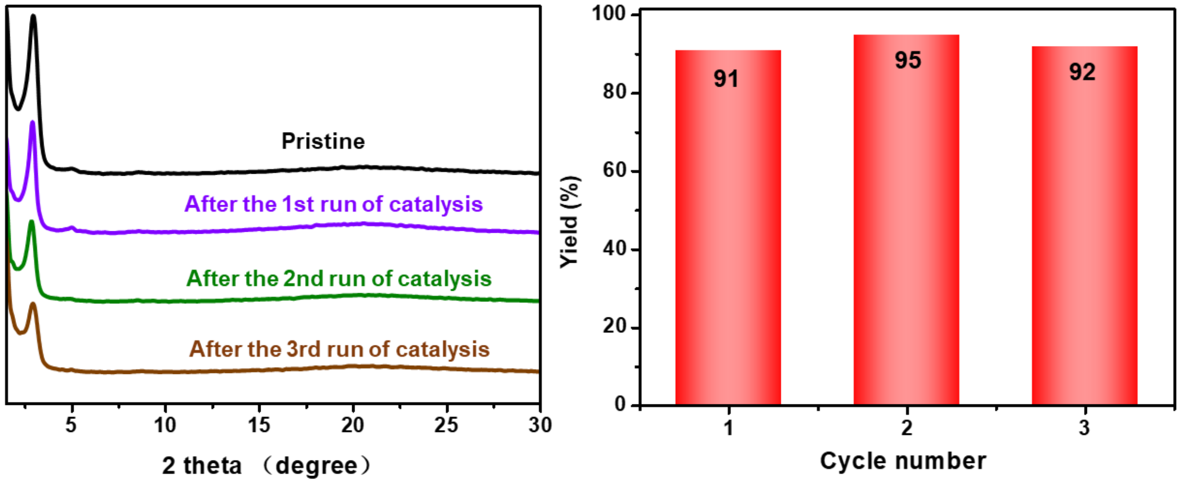

Figure S44 The PXRD (left) patterns of **18C6-COF** through the 3 recycle tests, and the catalytic results (right) through the 3 recycle tests. Yield determined by GC.

Section 9. References

[1] X. Jiang, X. Yang, C. Zhao and L. Sun *J. Phys. Org. Chem*. **2009**, *22,* 1–8

[2] Z. Zhu and T. M. Swager. *Org. Lett*. **2001**, *3*, 3471-3474.

[3] (a) E. R. Tompkins and S. W. Mayer, *J. Am. Chem. Soc.* **1947.** *69*, 2859–2865; (b) F. Yan, H. C. Pei, Y. C. Pei, T. L. Li, J. X. Li, B. Q. He, Y. Cheng, Z. Y. Cui, D. F. Guo and J. Y. Cui, *Ind. Eng. Chem. Res.* 2015, **54**, 3473-3479.

Section 10. Solution ^1H and ^{13}C NMR spectra

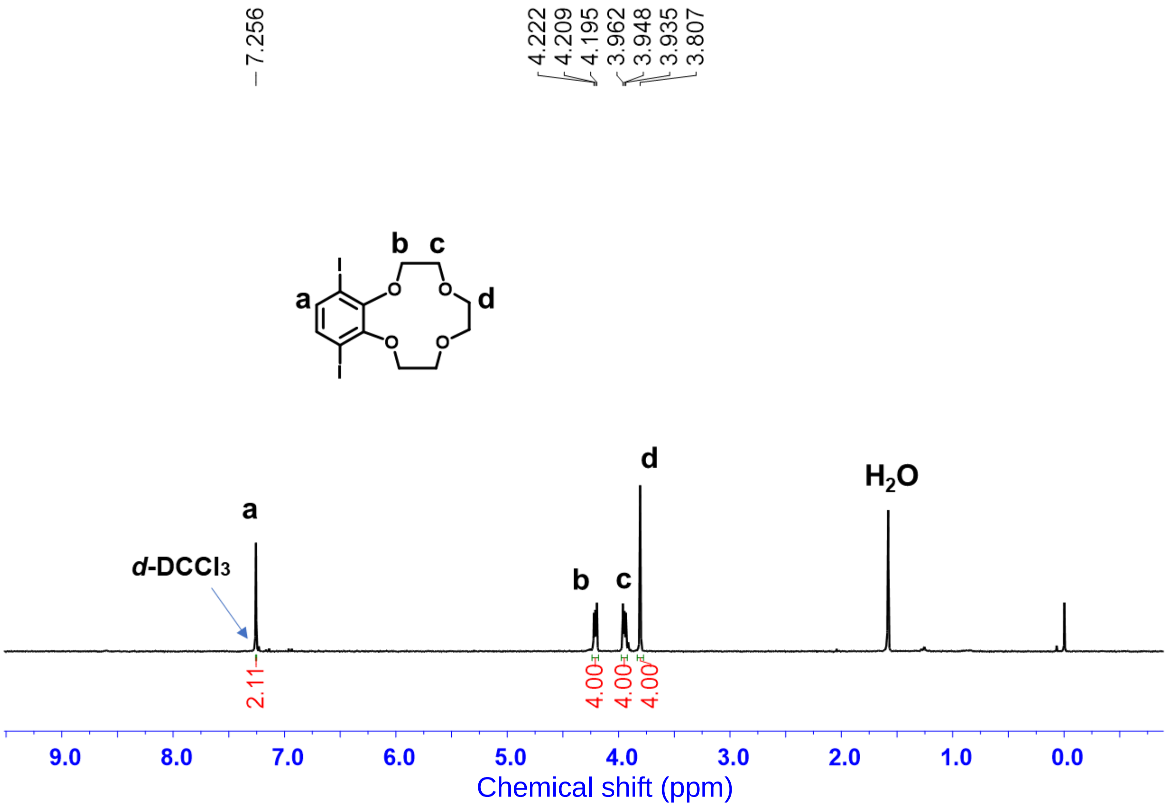

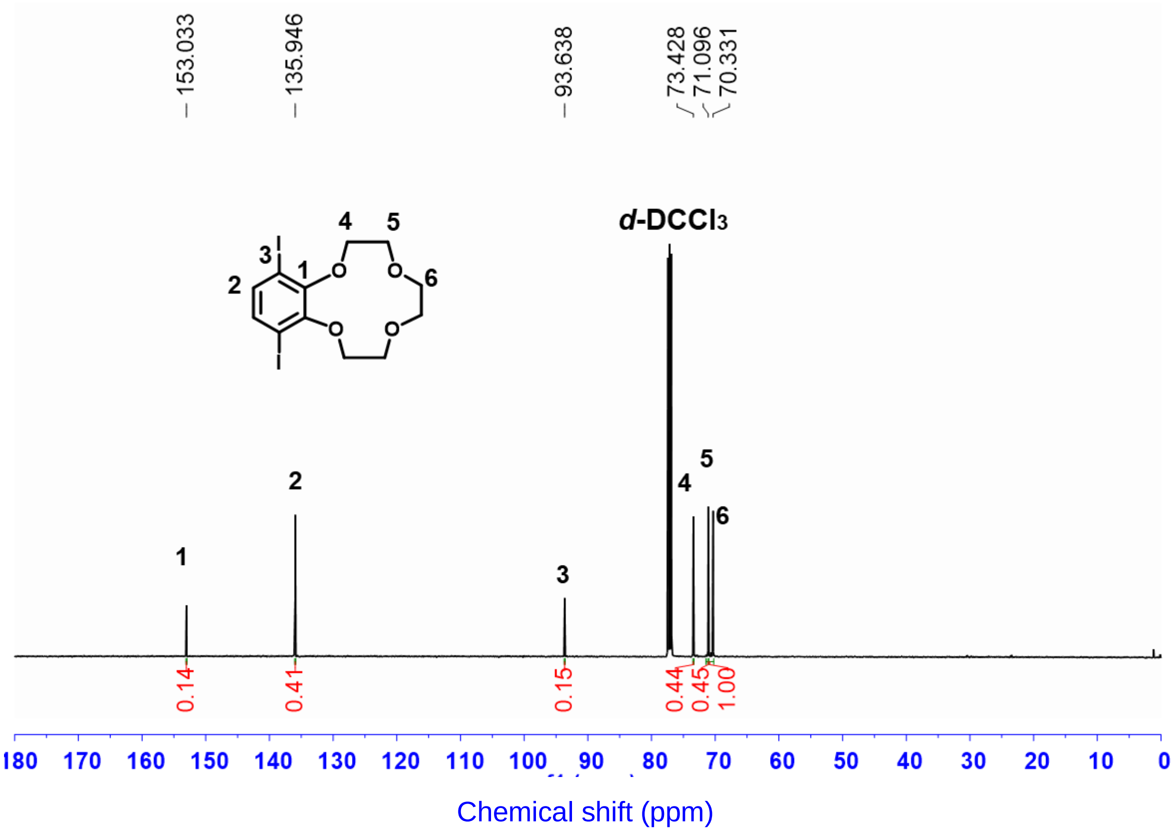

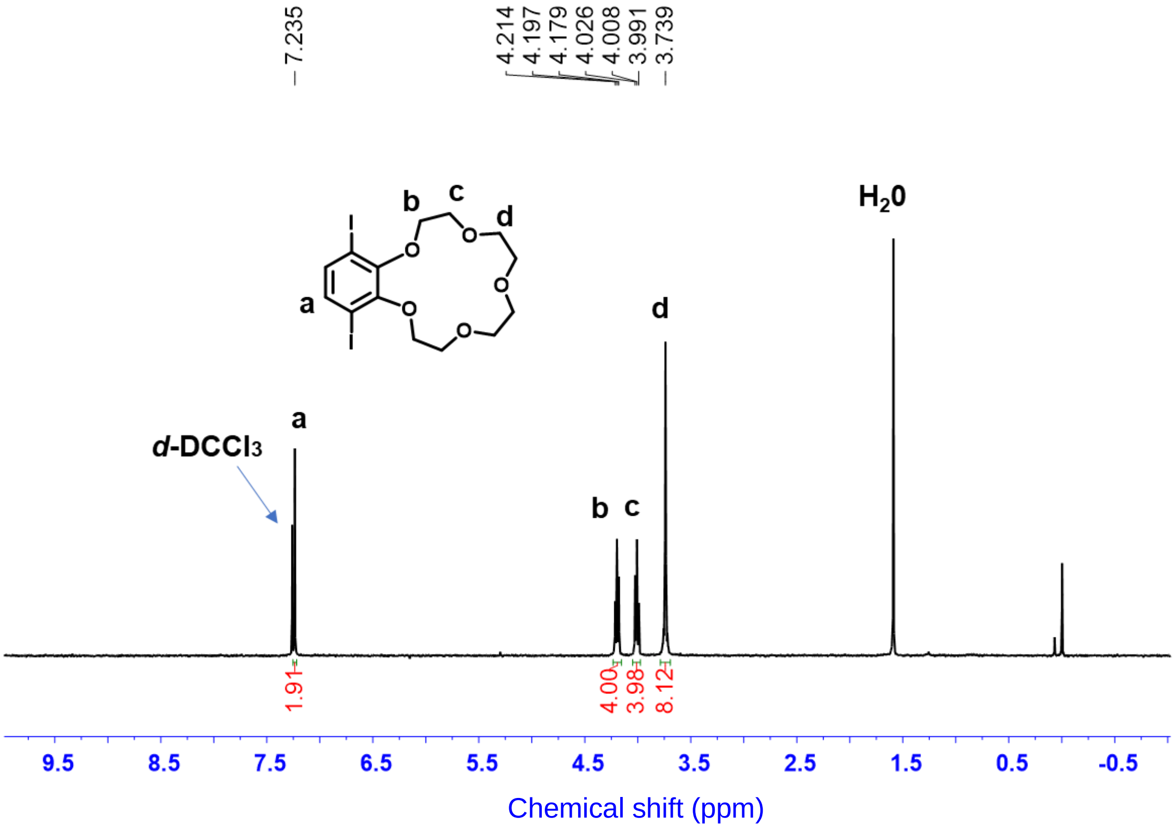
7.235
4.214
4.197
4.179
4.026
4.008
3.991
3.739
b
c
d
a
I
I
O
O
O
O
O
H$_2$0
d-DCCl3
a
d
b c
1.91
4.00
3.98
8.12
9.5
8.5
7.5
6.5
5.5
4.5
3.5
2.5
1.5
0.5
-0.5
Chemical shift (ppm)

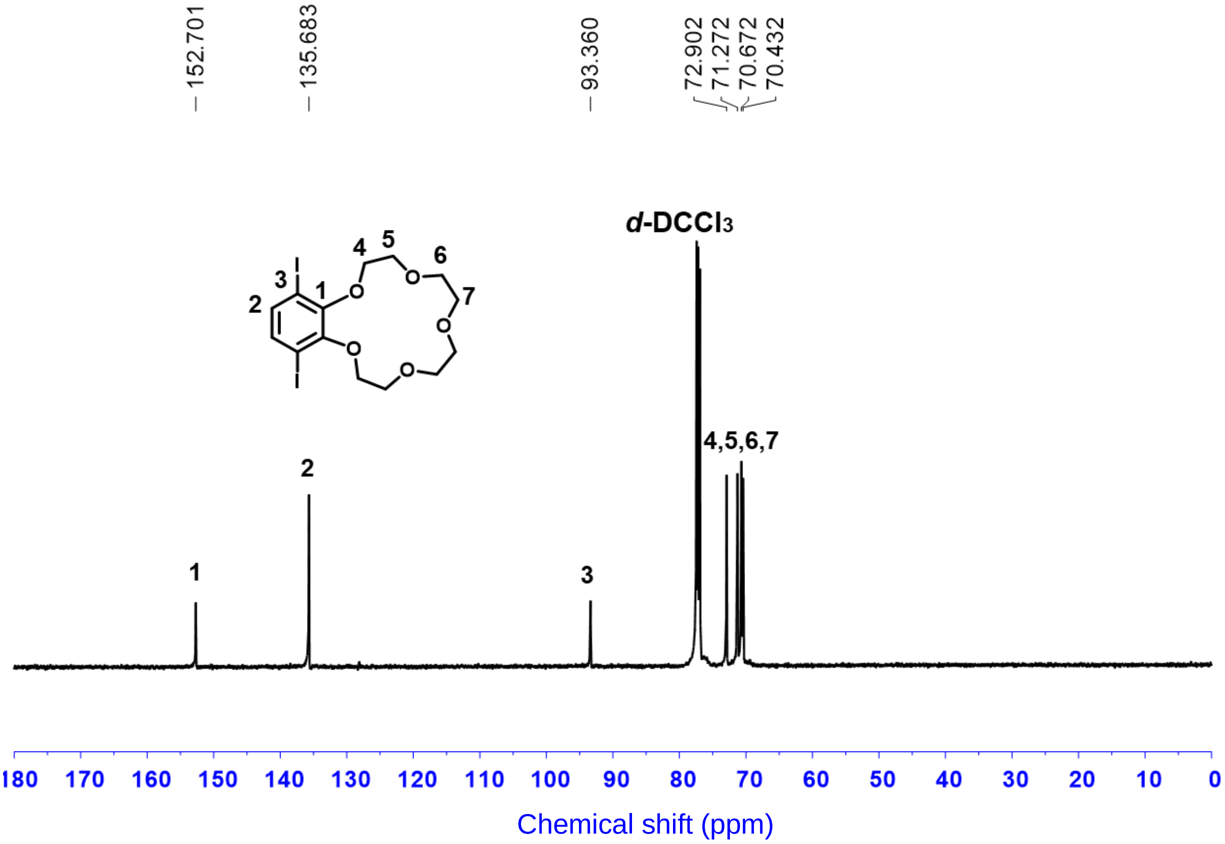
152.701
135.683
93.360
72.902
71.272
70.672
70.432
4
5
6
3
1
2
7
I
I
O
O
O
O
O
d-DCCl3
4,5,6,7
2
1
3
180
170
160
150
140
130
120
110
100
90
80
70
60
50
40
30
20
10
0
Chemical shift (ppm)

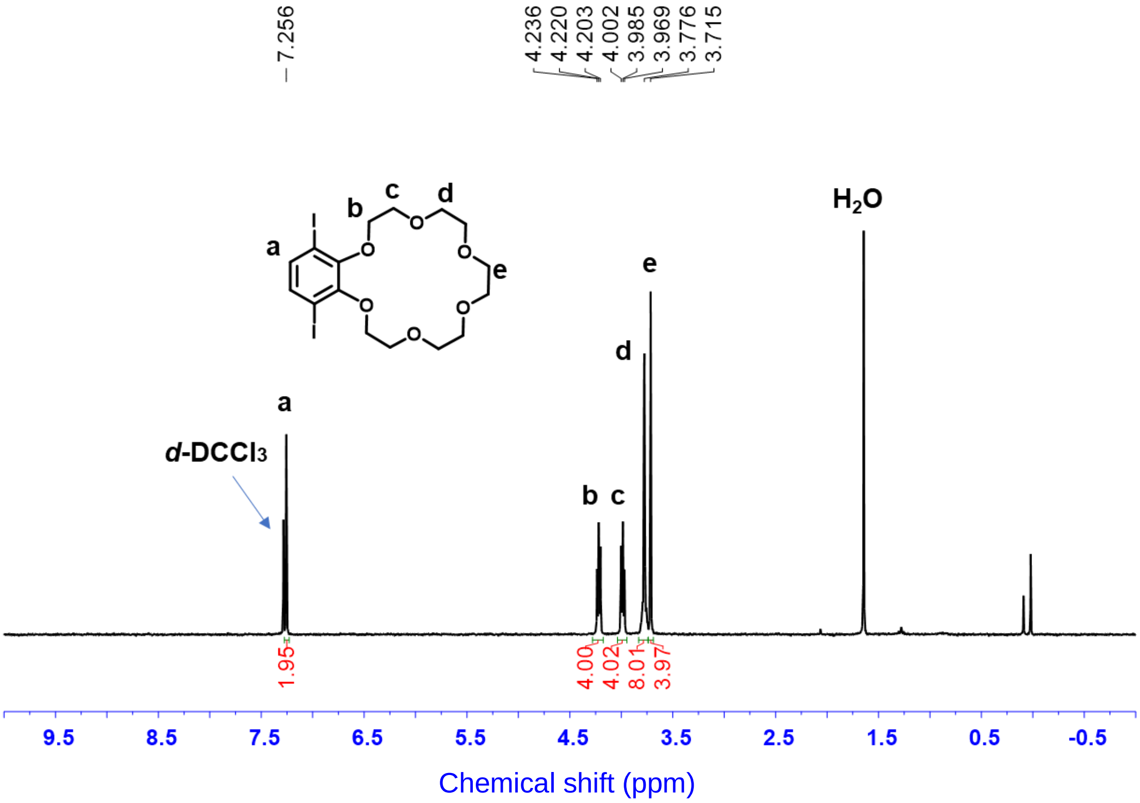
7.256
4.236
4.220
4.203
4.002
3.985
3.969
3.776
3.715
a
b
c
d
e
I
O
H$_2$O
d-DCCl3
1.95
4.00
4.02
8.01
3.97
9.5
8.5
7.5
6.5
5.5
4.5
3.5
2.5
1.5
0.5
-0.5
Chemical shift (ppm)

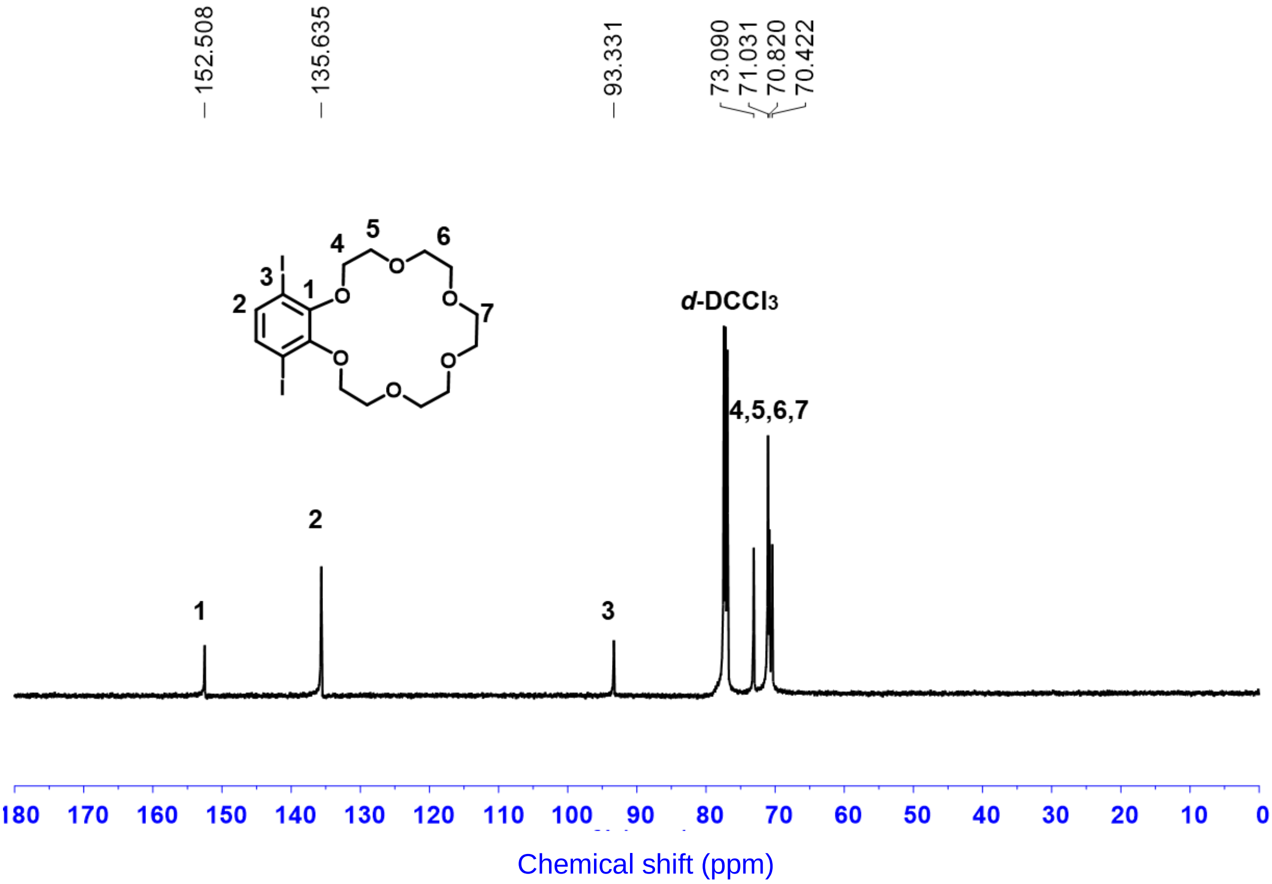
152.508
135.635
93.331
73.090
71.031
70.820
70.422
1
2
3
4
5
6
7
I
O
d-DCCl3
4,5,6,7
180
170
160
150
140
130
120
110
100
90
80
70
60
50
40
30
20
10
0
Chemical shift (ppm)

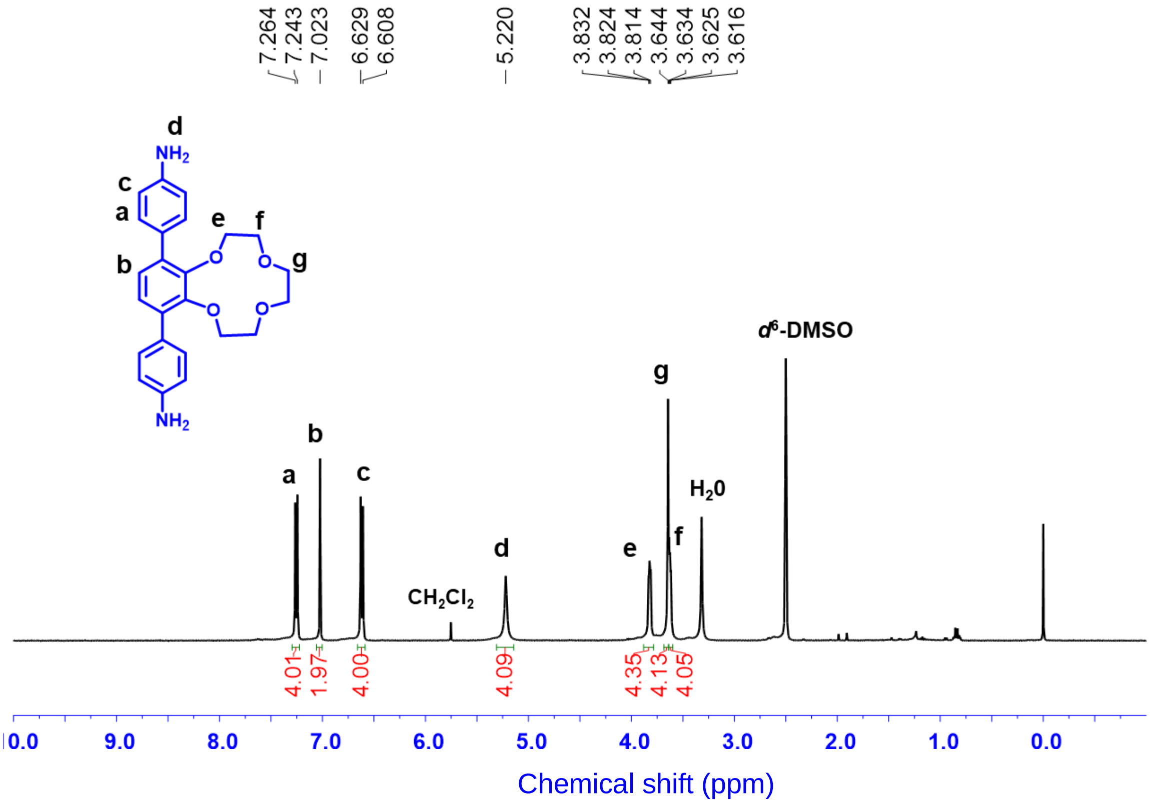
7.264
7.243
7.023
6.629
6.608
5.220
3.832
3.824
3.814
3.644
3.634
3.625
3.616
d
NH_2
c
a
e
f
g
b
NH_2
d^6-DMSO
g
b
a
c
H_20
f
d
e
CH_2Cl_2
4.01
1.97
4.00
4.09
4.35
4.13
4.05
10.0
9.0
8.0
7.0
6.0
5.0
4.0
3.0
2.0
1.0
0.0
Chemical shift (ppm)

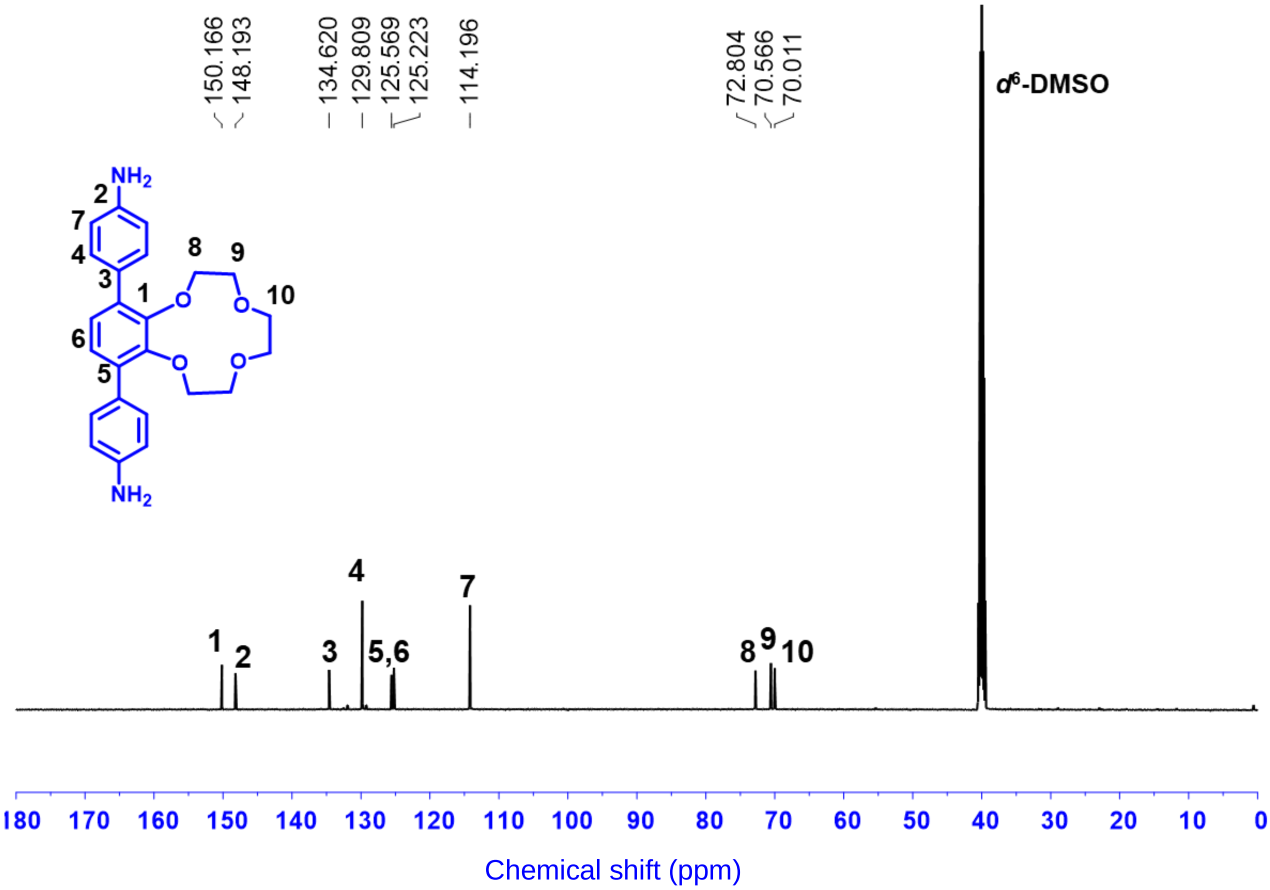
150.166
148.193
134.620
129.809
125.569
125.223
114.196
72.804
70.566
70.011
d^6-DMSO
NH_2
2
7
4
3
1
8
9
10
6
5
NH_2
4
7
1
2
3
5,6
8
9
10
180
170
160
150
140
130
120
110
100
90
80
70
60
50
40
30
20
10
0
Chemical shift (ppm)

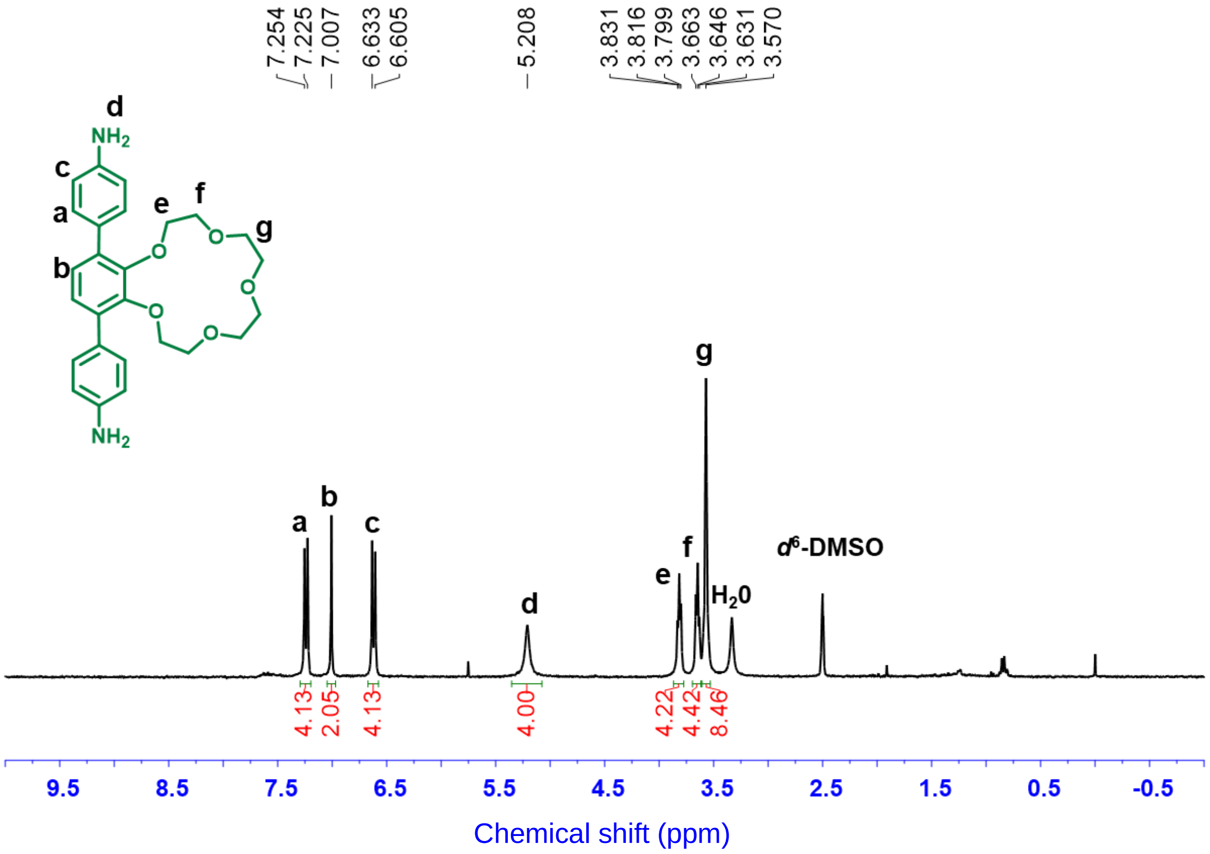
7.254
7.225
7.007
6.633
6.605
5.208
3.831
3.816
3.799
3.663
3.646
3.631
3.570
d
NH2
c
a
e
f
g
b
NH2
g
a
b
c
d
e
f
H20
d6-DMSO
4.13
2.05
4.13
4.00
4.22
4.42
8.46
9.5
8.5
7.5
6.5
5.5
4.5
3.5
2.5
1.5
0.5
-0.5
Chemical shift (ppm)

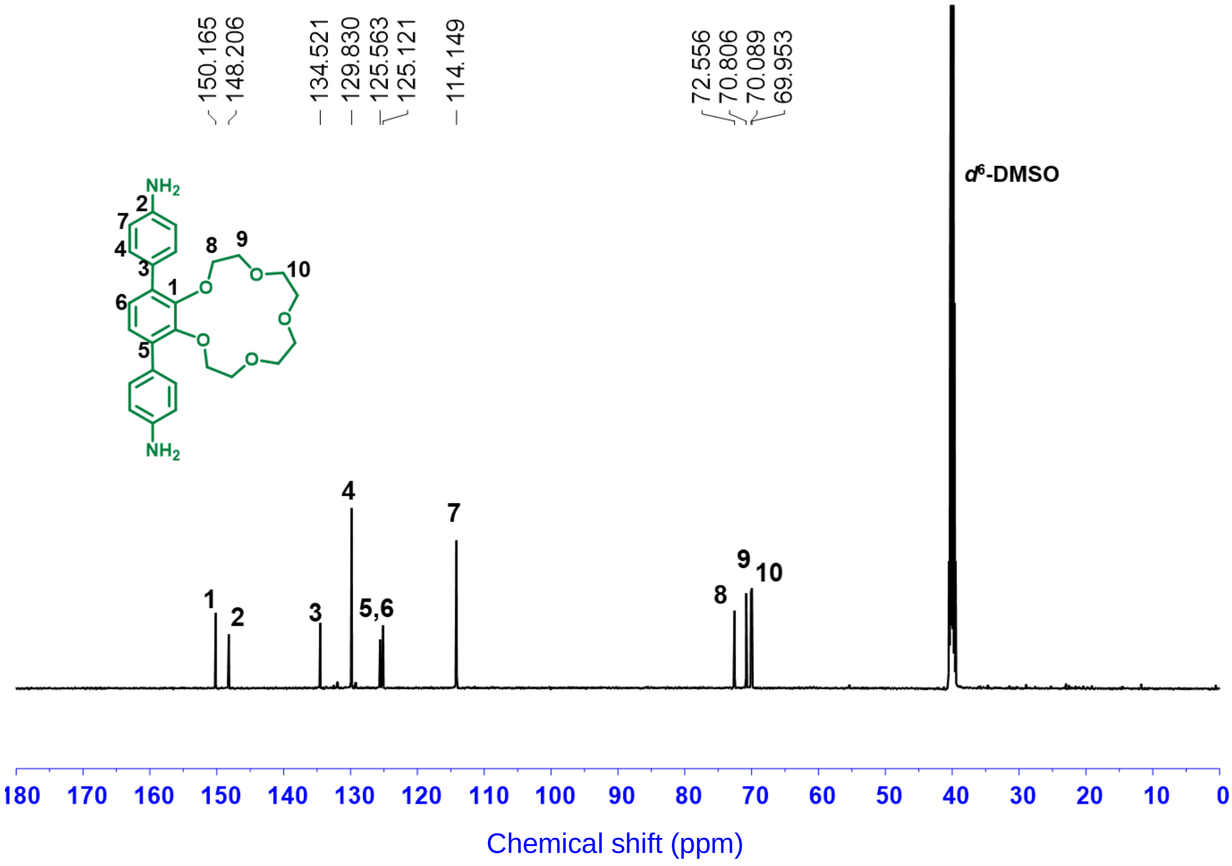
150.165
148.206
134.521
129.830
125.563
125.121
114.149
72.556
70.806
70.089
69.953
d6-DMSO
NH2
2
7
4
3
8
9
10
6
1
5
NH2
1
2
3
4
5,6
7
8
9
10
180
170
160
150
140
130
120
110
100
90
80
70
60
50
40
30
20
10
0
Chemical shift (ppm)

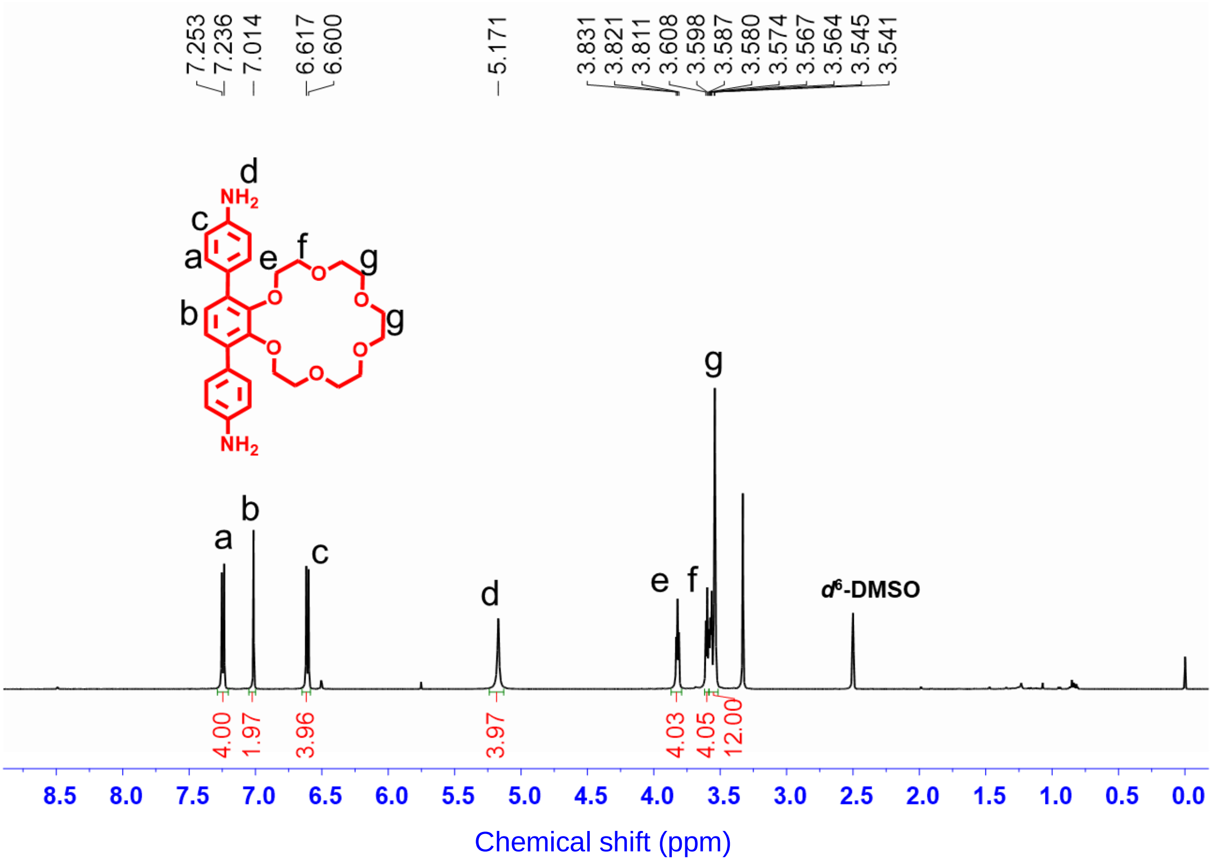
7.253
7.236
7.014
6.617
6.600
5.171
3.831
3.821
3.811
3.608
3.598
3.587
3.580
3.574
3.567
3.564
3.545
3.541
d
NH$_2$
c
a
e
f
g
b
g
NH$_2$
g
a
b
c
d
e
f
d^6-DMSO
4.00
1.97
3.96
3.97
4.03
4.05
12.00
8.5
8.0
7.5
7.0
6.5
6.0
5.5
5.0
4.5
4.0
3.5
3.0
2.5
2.0
1.5
1.0
0.5
0.0
Chemical shift (ppm)

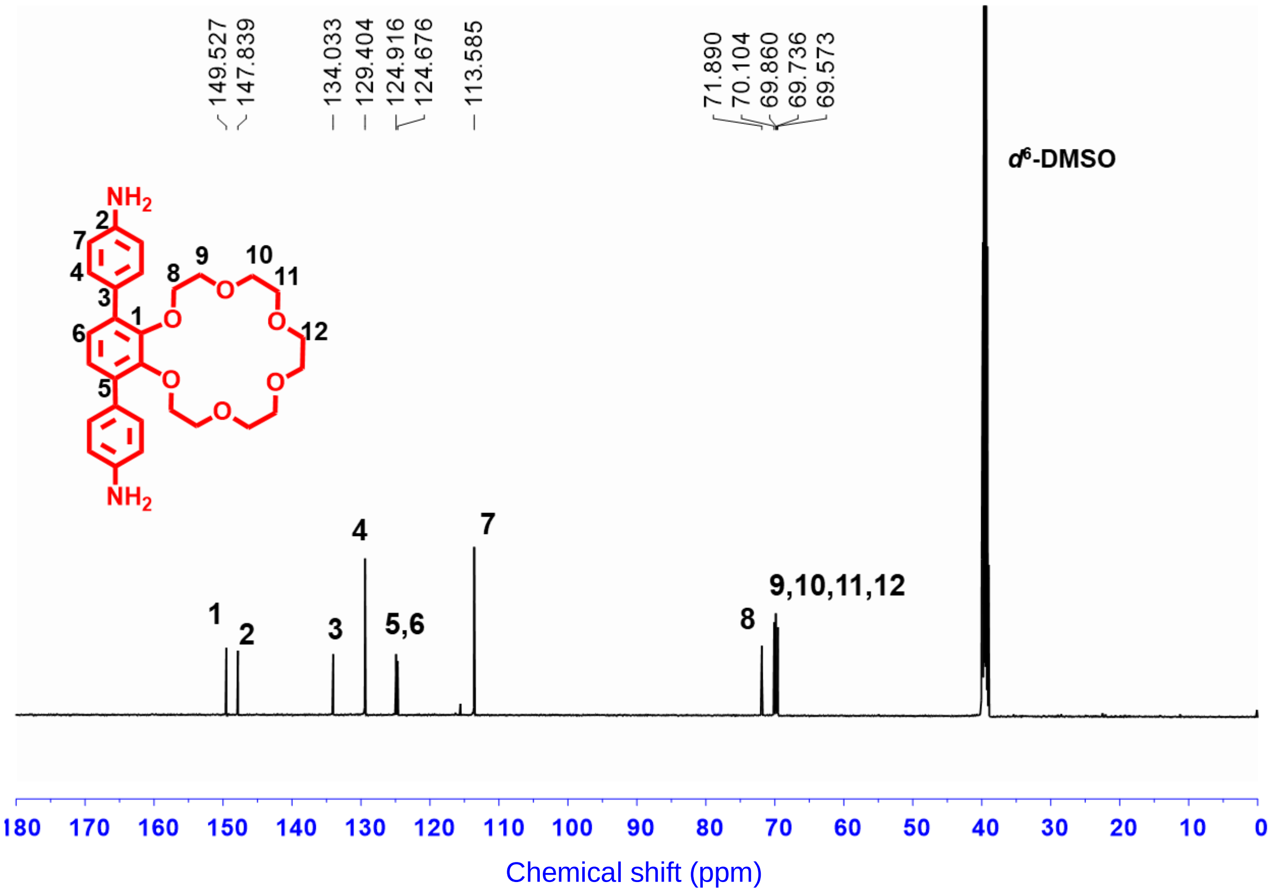
149.527
147.839
134.033
129.404
124.916
124.676
113.585
71.890
70.104
69.860
69.736
69.573
d^6-DMSO
NH$_2$
2
7
4
3
1
6
5
8
9
10
11
12
NH$_2$
1
2
3
4
5,6
7
8
9,10,11,12
180
170
160
150
140
130
120
110
100
90
80
70
60
50
40
30
20
10
0
Chemical shift (ppm)